

Open-Canopy: Towards Very High Resolution Forest Monitoring

Fajwel Fogel⁴ Yohann Perron^{3,5} Nikola Besic² Laurent Saint-André⁷
 Agnès Pellissier-Tanon¹ Martin Schwartz¹ Thomas Boudras¹ Ibrahim Fayad^{1,6}
 Alexandre d’Aspremont^{4,6} Loic Landrieu³ Philippe Ciais¹
¹ LSCE/IPSL, CEA-CNRS-UVSQ ² LIF, IGN, ENSG ³ LIGM, Ecole des Ponts, IP Paris CNRS, UGE
⁴ CNRS & École Normale Supérieure ⁵ EFEO ⁶ Kayrros ⁷ INRAE, BEF

Abstract

Estimating canopy height and its changes at meter resolution from satellite imagery is a significant challenge in computer vision with critical environmental applications. However, the lack of open-access datasets at this resolution hinders the reproducibility and evaluation of models. We introduce Open-Canopy, the first open-access, country-scale benchmark for very high-resolution (1.5 m) canopy height estimation, covering over 87,000 km² across France with 1.5 m resolution satellite imagery and aerial LiDAR data. Additionally, we present Open-Canopy- Δ , a benchmark for canopy height change detection between images from different years at tree level—a challenging task for current computer vision models. We evaluate state-of-the-art architectures on these benchmarks, highlighting significant challenges and opportunities for improvement. Our datasets and code are publicly available at [URL].

1. Introduction

Estimating canopy height at high spatial and temporal resolution is crucial for effective and responsive forest management [43, 69], conservation efforts, and policy-making in the face of climate change [18, 33, 42]. Meter-level spatial resolutions allow for identifying small vegetation structures, such as individual trees and understory vegetation [32], and for detecting local disturbances such as selective logging [3, 31]. Frequent temporal updates enable the monitoring of rapid changes in forest ecosystems [10, 52] caused by activities such as harvesting [75], illegal logging [35, 66], or wildfires, storms, and pest outbreaks [26]. This high granularity is essential for precise biomass estimation [64], biodiversity assessments [22], and understanding the ecological processes that occur on local scales [37].

Aerial Laser Scanning (ALS) provides precise measurements of canopy height [20], but its high cost and logistic requirements make frequent data acquisition impractical. In contrast, satellite images are abundant. A cost-effective alterna-

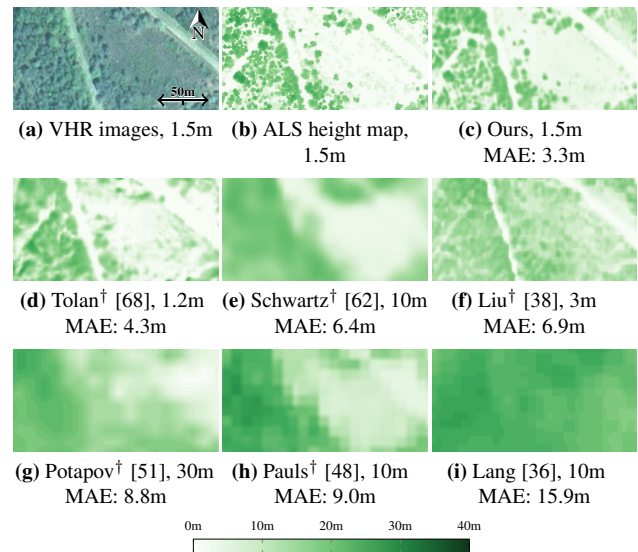


Figure 1. Canopy Height Estimation. We represent a VHR image from the Open-Canopy test set (a), alongside its corresponding ALS-derived canopy height (b). We include the height map estimated by a PVPTv2 [72] model trained on the Open-Canopy train set (c), compared against other canopy height products (d)-(i). For each image, we provide the spatial resolution of the evaluated map and its Mean Absolute Error. † the data or model used to generate these maps is not open-access.

tive to yearly ALS acquisition is to train models that estimate canopy height from a single Very High Resolution (VHR) satellite image using existing ALS data for supervision. Although recent studies have used VHR satellite images to predict canopy height [38, 68, 71] and published global height maps, their data and models are often not openly accessible. Many rely on commercial or closed data sources, require substantial pre-processing, and do not always disclose the location of their training sets (see Tab. 1).

To enable fair and reproducible evaluation of canopy height prediction models, we introduce Open-Canopy, the first entirely open-access benchmark for VHR canopy height estimation. Spanning over 87,000 km² across France, Open-Canopy combines SPOT 6-7 satellite imagery at 1.5m resolution with

Table 1. Canopy Height Prediction Datasets. We report information about the satellite images used as input, the canopy height used to train and evaluate models, and the number of ground truth (GT) data points (GEDI samples or ALS pixels). We group models by the resolution: Medium-to-High (\geq HR) and Very High Resolution (VHR).

Dataset	access			extent		images		height ground truth			direct download	commercial	complex pre-processing	special access	no train test split	S1 Sentinel-1	S2 Sentinel-2
	code	img	GT	scope	surface $\times 10^3 \text{ km}^2$	sensor	res. in m	sensor	res. in m	samples $\times 10^6$							
HR ^	Schwartz [62]	✗	Ⓜ	Ⓜ	France	588	S1/S2	10	GEDI	25	90						
	Lang [36]	✓	Ⓜ	Ⓜ	Global	14k	S2	10	GEDI	25	600						
	Potapov [51]	✗	Ⓜ	Ⓜ	Global	150k	Landsat	30	GEDI	25	372						
	Pauls [48]	✓	Ⓜ	Ⓜ	Global	2621	S1/S2	10	GEDI	25	Ⓜ						
VHR	Tolan [68]	✗	Ⓜ	Ⓜ	US	5.8	MAXAR	1.2	ALS+GEDI	1	5800						
	Wagner [71]	✗	Ⓜ	Ⓜ	US	3.8	NAIP	0.6	ALS	1	3784						
	Liu [38]	✗	Ⓜ	Ⓜ	Europe	700	Planet	3	ALS	3	77,777						
	Open-Canopy	✓	Ⓜ	Ⓜ	France	87	SPOT 6-7	1.5	ALS	1.5	38,876						

aerial LiDAR data at densities superior to 10 points/m², providing a rich dataset for training and evaluating machine learning models. Compared to datasets with similar accessibility [36], Open-Canopy improves the resolution of images by a factor of 6 and the height supervision by a factor of 16. Our downloadable dataset with ready-to-use training splits and data loaders aims at making forestry research more accessible to computer vision researchers.

In contrast to costly ALS measurements, satellite imagery can be acquired every year or less, and enables dynamic estimation of canopy height. This task is a major concern for both forest managers and authorities, as emphasized by recent European regulations [9] restricting the import of products related to deforestation. We introduce Open-Canopy- Δ , a subset of OpenCanopy with two consecutive ALS acquisitions. This data set allows us to formulate and benchmark the challenging problem of detecting dense forest height change, *i.e.* segmenting areas with a significant reduction in canopy height between two VHR satellite images.

Although existing studies [36, 38, 48, 51, 62, 71] predominantly evaluate UNet-type architectures [58], predicting canopy height from a single image presents a particularly challenging computer vision task that differs from typical natural image analysis settings. The satellite viewpoint deviates from conventional depth estimation scenarios, the inclusion of the crucial near-infrared band complicates the adaptation of RGB-based foundation models, and capturing the intricate relationships between tree radiometry, phylogeny, and allometry is difficult. In this paper, we evaluate a wide range of modern architectures and models, identify their current limitations, and present this task as a newly accessible, high-impact challenge for the computer vision community. Our contributions are as follows:

- **Open-Canopy:** An open-access dataset for canopy height estimation from VHR images with ALS annotations.

- **Open-Canopy- Δ :** An open-access dataset for segmenting canopy height changes between two images.
- **Benchmark:** An evaluation of recent computer vision architectures, foundation models, and forest products for these two tasks.

2. Related Work

This section details existing datasets and methods for the problem of canopy height estimation, grouped by annotation type: GEDI or ALS. See Tab. 1 for an exhaustive comparison of Open-Canopy with these datasets.

GEDI-Based Datasets. The Global Ecosystem Dynamics Investigation (GEDI) mission consists of a LiDAR mounted on the ISS and provides global canopy height measurements with a footprint diameter of 25m [15]. GEDI captures a set of spatially discrete full waveform echoes along paths approximately 4km wide. Models trained with GEDI data use it as a sparse and coarse supervisory signal to predict canopy height from medium to high resolution imagery such as Landsat images at 30m resolution (Potapov *et al.* [51]) or Sentinel-2 at 10m resolution (Schwartz *et al.* [62], Pauls *et al.* [48] and Lang *et al.* [36]). However, GEDI’s full waveform LiDAR can exhibit registration errors of up to 10m [60].

ALS-Based Datasets. Aerial Laser Scanning (ALS) uses low-flying aircraft equipped with LiDAR to create dense 3D point clouds of the Earth’s surface. These systems typically capture data at resolutions ranging from 10 to 60 points per square meter. This data is then rasterized along a high resolution grid, and used to estimate canopy height by subtracting the lowest quantiles height (ground surface) from the height of the highest quantiles (top of canopy). This allows the computation of “true” height maps which are then used to train models to predict canopy height from VHR images, at scales such as 1.2m for Tolan *et al.* [68] and Wagner *et al.*

[71], and 3m for Liu *et al.* [38]. Open-Canopy uses ALS data from the LiDAR-HD [29] program rasterized at 1.5m.

Canopy Height Estimation Models. Most canopy height prediction models employ fully supervised UNets [58] for their ease of use. The recent work by Tolan *et al.* [68] uses a Vision Transformer (ViT) [14] pretrained in a self-supervised fashion [47] on 18 million images without ALS height data. In this paper, we benchmark a variety of modern deep learning architectures for dense prediction of VHR canopy height from SPOT images, including Unet [58], Vision Transformers (ViT) [14], and their hierarchical variants [8, 39, 72]. We also explore how their pretraining impacts their ability to adapt from vision-related problems to the completely different task of canopy height estimation.

Canopy Height Change Estimation. As forests experience rapid losses [24, 40], better understanding and monitoring of forest dynamics is critical [41]. Although existing studies have explored the long-term evolution of forests [50, 53, 74], they focus on environmental or phenological variables and low-resolution (500m) images [56]. Models aiming to detect forest changes from images generally operate at medium or high resolution images (10-30m) [12, 16, 70]. Some work have explored the use of ALS [76] or drones [77], but typically operate over small areas and do not provide open-access data or code. To the best of our knowledge, Open-Canopy- Δ is the first open-access VHR benchmark for canopy height change detection with LiDAR-derived ground truth.

Data Access Policies. The seven studies in Tab. 1 all provide open-access predicted canopy height maps and often their trained models. However, only the work of Lang *et al.* provides its code and direct download links for their processed datasets. In contrast, the datasets used by Tolan *et al.*, Wagner *et al.*, and Liu *et al.* involve commercial satellite imagery or data that requires special access and cannot be redistributed. Although GEDI, Sentinel, and Landsat data are open-access, their preprocessing necessitates substantial expertise [65, 67]. Except for the studies of Tolan *et al.* and Lang *et al.*, these works also do not specify their training and testing splits, complicating their evaluation on external datasets due to potential overlap. Like the study of Lang *et al.*, our data, code, splits, and models are freely available. This transparency is crucial for advancing canopy height estimation as a mainstream application of vision models.

3. The Open-Canopy Benchmark

We introduce Open-Canopy, an open-access country-scale benchmark for estimating canopy height at very high resolution. We first present our dataset (Sec. 3.1), then the models evaluated (Sec. 3.2), and finally the results (Sec. 3.2) and limitations (Sec. 3.4) of the benchmark.

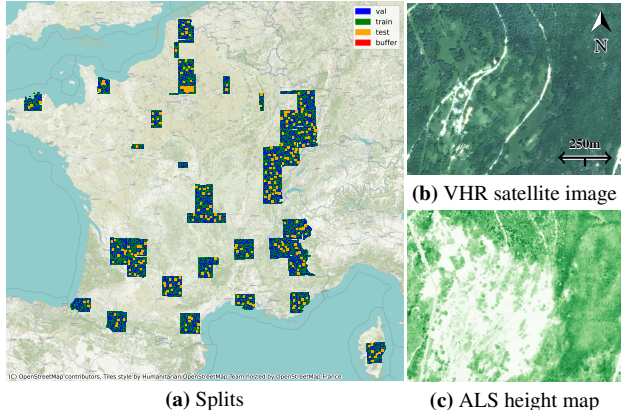


Figure 2. Open-Canopy. Our training, validation, and test sets span the French territory and use a 1km buffer (a). We provide VHR images at a 1.5 m resolution (b) and associated LiDAR-derived canopy height maps (c).

3.1. Dataset Characteristics

We explain here the main characteristics of the dataset of the Open-Canopy benchmark. We report a detailed description of the dataset construction in the supplementary material.

Why Just France? France offers a unique opportunity for developing an open-access, very high-resolution canopy height benchmark due to recent national initiatives that have made critical data sources publicly available under the open EtaLab2.0 license [17]: (i) DINAMIS [13] provides SPOT 6-7 very high-resolution (VHR) satellite imagery covering the entire French territory at a native panchromatic resolution of 1.5 m; and (ii) the LiDAR-HD project [29] offers extensive airborne 3D point clouds with densities exceeding 10 points per square meter. While other countries provide open-access ALS data [19, 46] and associated VHR images [44, 45], they are local solutions. SPOT 6-7 images provide consistent global coverage and make an excellent test bed for estimating the relevance of meter-scale satellite imagery. Moreover, the French metropolitan territory exhibits a wide range of climates—12 of the 18 Köppen-Geiger climate types found in continental Europe [49], including temperate, Mediterranean, and Alpine environments. The French forest inventory lists 190 distinct tree species [28]. While models trained on the Open-Canopy dataset may not generalize globally, their performance within Europe is likely to be robust given this environmental diversity.

Preprocessing. We have compiled over 100,000 km² of data from different providers. Despite advancements in geo libraries and government APIs, downloading, processing, and curating data required manual intervention, the development of custom functions, and significant computation. Deriving the canopy height from the ALS 3D point clouds alone took over 100 hours of continuous computation on a dedicated cluster with 70 CPUs. To facilitate future ex-

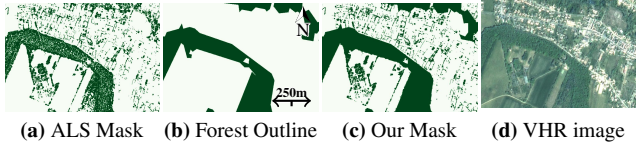


Figure 3. Vegetation Mask. We combine an ALS-derived vegetation mask (a) with official forest outlines (b) to build a pixel-precise mask (c) covering a wide range of vegetation types, as seen in the VHR image (d).

tensions of OpenCanopy, we provide scripts on our online repository to streamline these processes.

Extent and Splits. We selected 87,383 tiles across France, each measuring $1 \times 1 \text{ km}^2$. We divided the dataset into training ($66\,339 \text{ km}^2$), validation ($7\,369 \text{ km}^2$), and test sets ($13\,675 \text{ km}^2$). We added a 1 km buffer ($8\,046 \text{ km}^2$) between the test split and other splits to avoid data contamination, and ensured a representative distribution of each split among all bioclimatic regions of France [1].

VHR Satellite Images. As illustrated in Fig. 2(b), we use orthorectified SPOT 6-7 images [63, 73] from DINAMIS [13] with four spectral bands: red, green, blue, and near-infrared at a resolution of 6m, and a panchromatic band at a resolution of 1.5m. We apply pansharpening with the weighted Brovey algorithm [23] to upsample all four spectral bands to a resolution of 1.5m. We select images from the same year as the corresponding ALS acquisition campaign, in 2021, 2022 and 2023.

ALS-Based Canopy Height. As depicted in Fig. 2(c), we use ALS data from the LiDAR-HD project [29] between 2021 and 2023, which provides a minimum density of 10 points per m^2 . The canopy height maps are calculated at the same resolution as the VHR images by taking the maximum height difference between each point and its nearest *ground* point within each pixel. We interpolate ground height when necessary to be robust to very dense canopies. As described in the supplementary material, we validated the obtained canopy height maps by comparing them at both plot and tree-level with extensive in-situ measurements.

Vegetation Mask. As illustrated in Fig. 3, we construct a comprehensive vegetation mask by taking the union of the ALS-derived mask indicating vegetation over 1.5m in height, with official forest plots outlines, both provided by IGN [29, 30]. The resulting vegetation mask, covering 49% of the dataset, contains trees and shrubs both within forest plots and in other areas such as hedges and urban environments. This offers a more comprehensive evaluation area than the traditionally used forest boundaries [62].

3.2. Evaluated Models

We evaluate different state-of-the-art computer vision approaches for canopy height estimation from a single VHR satellite image with 4 spectral bands. We list below the selected models and how we adapted them to our task.

Selected Models. Given the ubiquity of convolutional models for canopy height estimation, we evaluate the **UNet** [58] and **DeepLabv3** [6] architectures. We select Vision Transformers (**ViT**) and their convolutional-hybrid variant (**HViT**) [14], as they recently became standard in computer vision. We also explore hierarchical ViT architectures such as **SWIN** [39], **PCPVT** [8], and **PVTv2** [72].

To assess the impact of pretraining, we include models pretrained on **ImageNet** [57, 57], but also large external datasets such as **DinoV2** [47] and **CLIP-OPENAI** [54]. We also consider the **ScaleMAE** [55] model, pretrained on satellite imagery of various resolutions, and Tolan *et al.*'s model [68] for canopy height estimation from RGB images.

Adapting Models. We adapt the architecture of the considered models, originally designed for the semantic segmentation of RGB images, to our setting. To handle the near-infrared channel, we change their input size from 3 to 4. We retain the pretrained weights related to RGB, and initialize the near-infrared channel weights with small random values drawn from a normal distribution $\mathcal{N}(0, 0.01)$. We use a transposed convolution as a decoder to predict continuous canopy heights and use the L_1 norm as a loss function.

Dataloader and Evaluation. During training, we sample random tiles of size 224×224 pixels with data augmentation: random scaling from 0.5 to 2, and rotations 0, 90, 180, or 270° . For inference, we sample tiles on a regular grid of 112 pixels, and only keep the center half of each prediction of size 224×224 . We train our model to predict the canopy height for all pixels, which may not correspond to vegetation. However, we only compute the evaluation metrics for pixels within the vegetation mask described in Sec. 3.1.

Parameters and Resources. We use a batch size of 64 and the ADAM optimizer [34] with a learning rate of 10^{-3} , a linear warm-up of 1 epoch, and a ReduceLROnPlateau scheduler [2] with a patience of 1 and a decay of 0.5. We perform early stopping with a patience of 3. These hyperparameters were selected by considering their impact on the UNet and ViT models. Reproducing all our experiments requires 1400 GPU-h with A100 GPUs. We estimate our hyperparameters search and initial experiments to 2000 GPU-h.

3.3. Results and Analysis

We evaluate recent vision models in Tab. 2, as well as the accuracy of existing canopy height maps in Tab. 3.

Metrics. We evaluate the performance of canopy height esti-

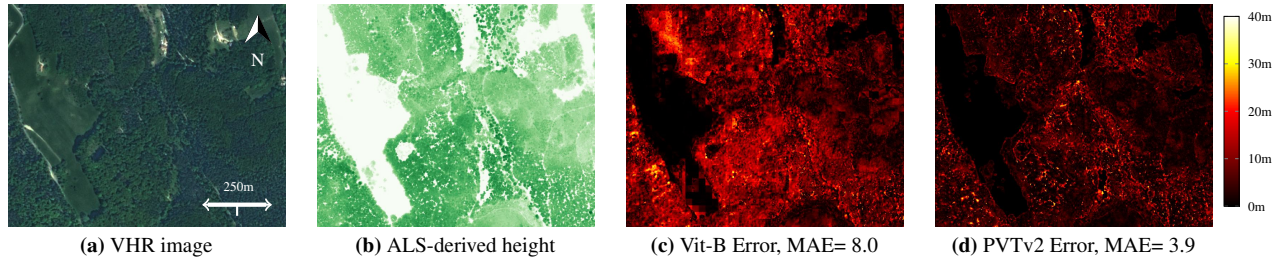


Figure 4. Difference Maps: Per-pixel absolute (top row) and relative (bottom row) errors for ViT-B and PVTv2. PVT2 predictions are more precise with errors mostly under 10m while Unet mispredict a lot of tree by more than 20m

Table 2. Canopy Height Prediction Models. We benchmark several backbone models for the task of predicting the canopy height of each pixel from a single satellite image. All models are pretrained on vision datasets and fine-tuned on our training set.

Model	pretraining	MAE in m	nMAE in %	RMSE in m	Bias in m	Tree cov. IoU in %
UNet ⁴ [58]	ImageNet1k [59]	2.67	23.8	4.18	-0.30	90.4
DeepLabv3 ¹ [6]	ImageNet1k [59]	3.18	28.4	4.83	-0.26	88.0
ViT-B ³ [14]	ImageNet21k [6]	4.26	37.8	6.06	-0.84	86.0
HViT ³ [14]	ImageNet21k [6]	2.65	24.0	4.18	-0.13	90.2
PCPVT ³ [8]	ImageNet1k [6]	2.57	23.1	4.06	-0.17	90.4
SWIN ³ [39]	ImageNet21k [6]	2.54	22.8	4.00	-0.11	90.5
PVTv2 ³ [72]	ImageNet1k [6]	2.52	22.9	4.02	0.00	90.5
ScaleMAE ⁵ [55]	FotM [7]	3.45	31.2	5.13	-0.48	88.2
ViT-B ³ [14]	DINOv2[47]	4.84	43.2	6.68	-0.48	84.8
ViT-B ² [14]	CLIP_OPENAI [54]	2.87	25.9	4.43	-0.07	89.7
ViT-L ⁶ [14]	Tolan[68]	4.46	38.9	6.27	-1.03	85.6
SWIN ³ [39]	Satlas-pretrained [4]	2.56	23.1	4.09	0.02	90.6

¹pytorch.org/vision ²huggingface.co/laion ³timm.fast.ai/ ⁴github.com/qubvel/segmentation_models.pytorch
⁵github.com/bair-climate-initiative/scale-mae ⁶github.com/facebookresearch/HighResCanopyHeight

mation models with five metrics: Root Mean Square Error (**RMSE**), Mean Absolute Error (**MAE**), normalized MAE (**nMAE**)—which normalizes the absolute error by the target height, **Bias**—the error averaged across the test set, and Intersection over Union (IoU) for **Tree Cover** predictions. The tree cover IoU is calculated by comparing binary maps generated by thresholding both ground truth and predicted height maps at a 2m threshold. All metrics are computed only on pixels within the vegetation mask and with ground truth height below 60m. The nMAE is calculated only for pixels with ground truth heights above 2m.

Analysis. We report the quantitative performance of all evaluated backbones in Tab. 2, and selected illustrations in Fig. 4. We make the following observations:

- **Impact of Backbones.** Contrary to trends in natural image analysis, convolution-based approaches (UNet, HVIT) outperform ViTs, indicating that convolutions can more efficiently extract relevant local features than linear projections. However, hierarchical ViTs (SWIN, PCPVT, PVTv2) achieve the highest precision, under-

scoring the multi-scale structure of the task.

- **Impact of Pretraining.** Interestingly, models pretrained on ImageNet (UNet, PVTv2) perform better than foundation models trained on extensive databases of natural images (CLIP, DINO). These models do not generalize well to canopy height estimation, likely due to differences in viewpoint, task specificity, data type, and available spectral bands. Pre-training on satellite images does not either improve performance: a SWIN model pre-trained on the SATLAS dataset achieves similar performance as when pre-trained on ImageNet, while ScaleMAE, and Tolan *et al.*'s ViT [68] do not adapt well to our task. We hypothesize that this is due to the spatial domain shift and the fact that they are trained without the near-infrared channel. See the ablation experiments in the supplementary material for additional analysis.
- **Overall Performance.** The methods assessed in this benchmark exhibit commendable results, achieving tree cover detection with over 90% IoU and an nMAE of

Table 3. Canopy Height Maps Evaluation. We evaluate several available canopy height map products on our test set.

Map	Backbone	res. in m	MAE in m	nMAE in %	RMSE in m	Bias in m	Tree cov. IoU in %
Potapov [51]	UNet	30	6.27	58.1	8.68	1.79	78.0
Schwartz [61, 62]	UNet	10	5.17	42.7	7.20	3.37	76.8
Lang [36]	CNN	10	9.22	89.5	17.14	8.40	77.4
Pauls [48]	UNet	10	6.70	58.3	8.65	5.22	76.8
Liu [38]	UNet	3.0	4.83	46.6	6.90	1.56	84.1
Tolan [68]	ViT-L	1.0	5.07	43.7	7.15	-2.95	78.8
Open-Canopy	UNet	1.5	2.67	23.8	4.18	-0.30	90.4
Open-Canopy	PVTv2	1.5	2.52	22.9	4.02	0.00	90.5

around 20% for the best-performing models. However, we argue that there exists a significant margin of improvement, in particular for transferring foundation models to our setting.

Impact of Initialization. We report in Tab. 4 the performance of PVTv2 trained on ImageNet1k, our best performing model, when fine-tuned with different initialization strategies to accommodate the fourth near-infrared channel. Fully random initialization leads to poor performance, which shows that Open-Canopy is not large enough to train a ViT from scratch. LoRA [25] adaptation adapts better to the new channel, but fine-tuning all weights with a random first layer leads to significantly better results. Our proposed initialization scheme further improves the results by allowing the network to gradually accommodate the new channel.

Comparison with Existing Maps. In Tab. 3, we evaluate the precision of canopy height maps generated by UNet and PVTv2 networks trained on the Open-Canopy dataset against those from other research that we interpolate to a resolution of 1.5m per pixel. With the caveats on the fairness of the comparison mentioned in Sec. 3.4, our maps achieve significantly better precision. The low performance of models derived from low-resolution imagery is expected, as they are trained to estimate tree height at a different resolution. Among the ALS-based methods, Liu *et al.*'s model performs best, likely due to its training data from Europe, which differs from Tolan *et al.*'s training in the continental US. Moreover, the Tolan *et al.* model relies solely on RGB data, while the inclusion of near-infrared is proven to be highly discriminative for vegetation analysis [5]. In Fig. 5, we report error plots across various vegetation height bins, highlighting that the PVTv2 model trained on Open-Canopy exhibits significantly lower bias and superior performance, especially in areas with tall trees.

Out-of-domain Evaluation. To assess the spatial generalization of models trained on Open-Canopy, we collected

Table 4. Initialisation Strategy. We evaluate different training strategy for a PVTv2 model trained on ImageNet1k.

Initialization	MAE in m	nMAE in %	RMSE in m	Bias in m
Fully random	11.17	85.77	14.38	-10.94
LoRA (rank 4)	4.54	40.79	6.42	-0.37
Rand. 1st layer	2.87	24.3	4.24	-0.04
Proposed	2.52	22.9	4.02	0.00

SPOT 6-7 satellite imagery (with DINAMIS [13]) and aerial VHR images (through NAIP [44]) for a 30km² area in Utah, United States. We used as ground truth the ALS-based canopy height map provided by NEON on site REDB [19]. As detailed in Tab. 5, a PVTv2 model trained on Open-Canopy and applied to the SPOT image achieves performance comparable to Tolan *et al.*'s height map derived from MAXAR 0.6m imagery [68], despite their model being predominantly trained on data from the continental US. This demonstrates the robustness of models trained on Open-Canopy to evaluation outside of France.

We resampled NAIP aerial images to 1.5m resolution and normalized them with histogram matching to the global spectral distribution of the entire Open-Canopy dataset. Evaluated on these images, the performance of the PVTv2 model decreases starkly, highlighting its dependency on SPOT data.

3.4. Limitations

While Open-Canopy represents a significant advancement in providing an open-access VHR benchmark for canopy height estimation, it has several limitations.

- **Constraints of Open-Access:** Only using freely distributable sources limits the extent as well as the spatial and temporal resolution of available data. Acquiring and distributing ALS and VHR satellite images at large scale is cost-prohibitive: Open-Canopy would cost millions of dollars to reproduce with commercial data.

Table 5. Out-of-Domain Evaluation. We evaluate different models on a 30km² area in Utah, US. We compare the height map of Tolan *et al.* [68] to a PVTv2 model trained on Open Canopy with SPOT6-7 data or NAIP images.

	Input data	Training area	MAE in m	nMAE in %	RMSE in m	Bias in m	Tree cov. IoU in %
Tolan Map [68]	MAXAR	US	2.02	47.4	3.58	0.57	70.5
PVTv2	NAIP	OpenCanopy	4.38	71.0	6.42	2.78	49.6
PVTv2	SPOT 6-7	OpenCanopy	2.08	33.9	3.20	0.90	61.8

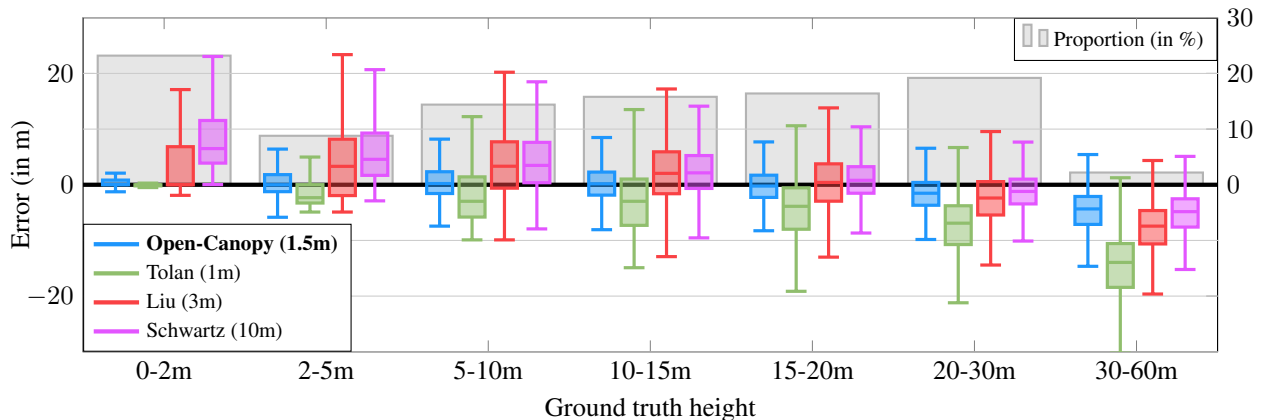


Figure 5. Distribution of Error. We plot the distribution of errors according to the ground truth canopy height for a PVTv2 model trained on Open-Canopy and different canopy height map products.

- **Geographic Scope:** Although metropolitan France offers a unique combination of open-access data and diverse landscapes, it lacks critical forest types such as rainforests. This absence may affect the generalizability of models trained on Open-Canopy. We hope that this work will inspire similar open-access initiatives in other countries, leading to the creation of a truly global VHR canopy height dataset.
- **Limits of ALS:** Our ground-truth canopy heights are derived from aerial LiDAR measurements, which can contain errors due to factors like multiple echoes. Although we estimate these errors with in-situ measurements (see the supplementary material), they cannot be entirely eliminated. Additionally, while the freely distributable SPOT 6-7 images are captured during spring and summer, the LiDAR measurements span all seasons. This temporal mismatch may encourage models to predict average heights rather than capturing seasonal variations.
- **Comparison with Other Products.** Our evaluation of other canopy height maps is subject to limitations: (i) unknown training sets for some models might lead to data contamination, (ii) interpolation might distort results, (iii) forest losses and gains happening between the timing of images and ALS acquisitions can affect performance, (iv) maps derived at lower resolution are

trained to predict the maximum canopy height in larger pixels, which bias them to higher values. To address these issues, we provide additional experiments in the supplementary material and openly release all related data to facilitate more accurate future evaluations.

4. Open-Canopy- Δ

We present Open-Canopy- Δ , a benchmark for canopy height change detection between consecutive VHR images. We describe the dataset in Sec. 4.1 and our results in Sec. 4.2.

4.1. Dataset Characteristics

Extent and Context. Open-Canopy- Δ focuses on the Forêt de Chantilly, a declining forest due to climate change and of high concern for conservationists [11]. We consider two ALS acquisitions in February 2022 [29] and September 2023 [11], allowing us to build two consecutive canopy height maps and collect corresponding SPOT 6-7 satellite images. The studied area spans 16,634 hectares and is strictly comprised in the test set of Open-Canopy, *not* overlapping with the training set.

Processing. We generated a rasterized canopy change map by subtracting the ALS-based height map of 2022 from the map of 2023. Significant decreases in canopy height can result from various forest disturbance events such as

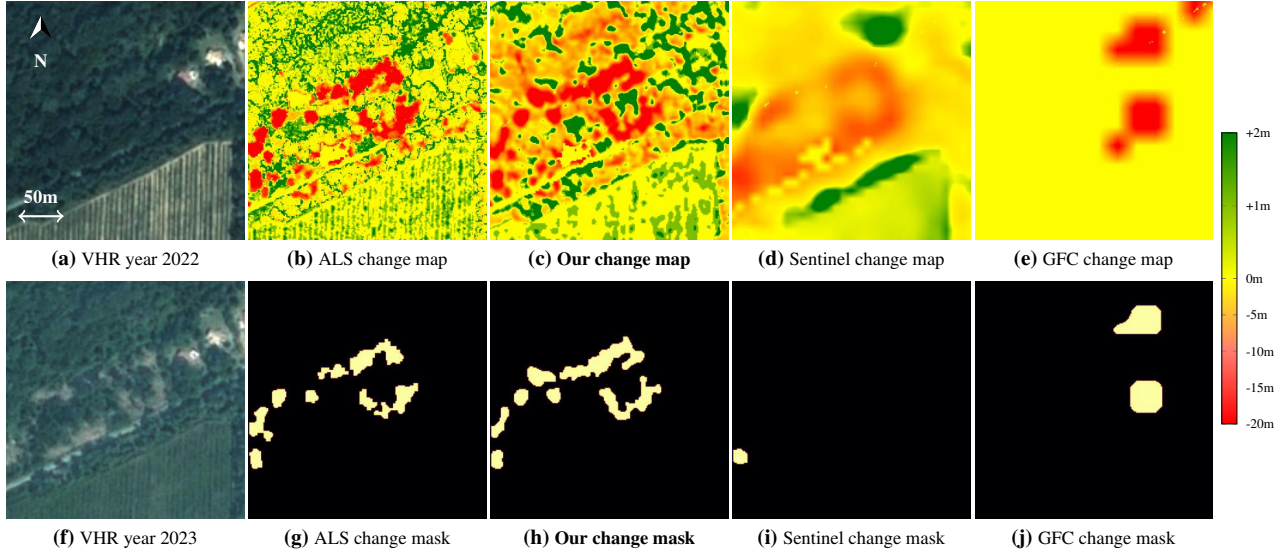


Figure 6. Canopy Height Change. We consider VHR images taken in the Chantilly Forest taken in 2022 (a) and 2023 (f), and use ALS observations of the same years to derive a canopy height change map (b). We represent the change map predicted by a PVTv2 model (c) and two competing approaches: Sentinel-derived maps from Schwartz *et al.* [62] (d) and Global Forest Change [24] (e). Finally, we compare the binary change masks derived from ALS measurements (g) and the predicted change maps (i),(h),(j).

fires, logging, diebacks, or maintenance activities. However, minor changes due to seasonal growth cycles, wind, or sensor errors can introduce noise. To create robust binary *change masks*, we focused on areas with substantial, localized, and consistent decreases in canopy height. The processing steps involve: (i) selecting pixels with a height loss exceeding 15m, (ii) applying erosion and dilation operators using a 3-pixel kernel to regularize the binary masks, and (iii) removing connected components smaller than 200m². Each of the resulting 73 change areas was manually validated by a forest expert, ensuring the quality and accuracy of the benchmark. We assigned zero values to false positive in the ALS change map. Illustrations, detailed explanations of hyperparameter choices and verification processes are provided in Fig. 6 and the supplementary material.

4.2. Results and Analysis

We evaluate different approaches for detecting significant canopy height change between two VHR images, a task which holds significant applications in forestry management and deforestation monitoring.

Setting. We provide each model images from 2022 and 2023 and generate two canopy height maps. We obtain a change map by taking the difference. We do not directly compare the ALS-derived and predicted change maps, as the estimation error of canopy height can be larger than normal tree growth. Instead, we apply the preprocessing described in Sec. 4.1 to produce a binary mask of predicted canopy height change.

Table 6. Forest Change Mask Evaluation. We evaluate our best model (PVTv2) for the task of canopy height change detection.

	Precision (%)	Recall (%)	F1 score (%)	IoU (%)
Schwartz [62]	63.5	3.2	6.0	3.1
GFC [24]	0.9	11.1	1.7	0.8
PVTv2 (ours)	53.8	54.3	54.1	37.0

Metrics. We evaluate the predicted canopy height change masks by computing the pixel-wise **Precision, Recall, F1 score**, and **IoU** with respect to the ALS-derived masks.

Results. We compare height change masks obtained with a PVTv2 model trained on Open-Canopy with those derived from height maps provided by [62] and Global Forest Change [24]. As detailed in Tab. 6, our model achieves significantly better performance than other methods. Fig. 6 illustrates that while our predicted change maps do not perfectly align with the ground truth maps, the consistency of our predictions suggests their potential utility in detecting significant year-to-year changes.

5. Conclusion

We introduced Open-Canopy, an open-access country-scale benchmark combining VHR satellite imagery with ALS-derived canopy height measurements. We evaluated multiple state-of-the-art computer vision models for canopy height estimation. Despite the dominance of convolutional net-

works in prior works, our findings suggest that transformer-based architectures exhibit superior performance. We also proposed Open-Canopy- Δ , a benchmark for canopy height change detection in consecutive observations, a difficult task, even for the best-performing models. We hope that our open-access benchmarks will encourage the computer vision community to further explore canopy height estimation as a standard task for evaluating new architectures and inspire forestry experts to design bespoke architectures.

References

- [1] Fiches descriptives des grandes régions écologiques (GRECO) et des sylvoécorégions (SER). <https://inventaire-forestier.ign.fr/spip.php?article773>. Accessed: 2024-04-29.
- [2] PyTorch: ReduceLROnPlateau. [org/docs/stable/generated/torch.optim.lr_scheduler.ReduceLROnPlateau.html#torch.optim.lr_scheduler.ReduceLROnPlateau](https://pytorch.org/docs/stable/generated/torch.optim.lr_scheduler.ReduceLROnPlateau.html#torch.optim.lr_scheduler.ReduceLROnPlateau). Accessed: 2024-02-29.
- [3] Gregory P Asner, Michael Keller, Rodrigo Pereira, Jr, Johan C Zweede, and Jose NM Silva. Canopy damage and recovery after selective logging in Amazonia: Field and satellite studies. *Ecological Applications*, 2004.
- [4] Favien Bastani, Piper Wolters, Ritwik Gupta, Joe Ferdinando, and Aniruddha Kembhavi. Satlaspretrain: A large-scale dataset for remote sensing image understanding. In *ICCV*, pages 16726–16736, 2023.
- [5] Toby N Carlson and David A Ripley. On the relation between NDVI, fractional vegetation cover, and leaf area index. *Remote sensing of Environment*, 1997.
- [6] Liang-Chieh Chen, George Papandreou, Florian Schroff, and Hartwig Adam. Rethinking atrous convolution for semantic image segmentation. *arXiv preprint arXiv:1706.05587*, 2017.
- [7] Gordon Christie, Neil Fendley, James Wilson, and Ryan Mukherjee. Functional map of the world. In *CVPR*, 2018.
- [8] Xiangxiang Chu, Zhi Tian, Yuqing Wang, Bo Zhang, Haibing Ren, Xiaolin Wei, Huaxia Xia, and Chunhua Shen. Twins: Revisiting the design of spatial attention in vision transformers. *NeurIPS*, 2021.
- [9] European Commission. Regulation on deforestation-free products. https://environment.ec.europa.eu/topics/forests/deforestation/regulation-deforestation-free-products_en, 2024. [Online; accessed 12-Sep-2024].
- [10] Adrian J Das and Nathan L Stephenson. Improving estimates of tree mortality probability using potential growth rate. *Canadian Journal of Forest Research*, 2015.
- [11] Institut de France. Collectif sauvons la forêt de chantilly. <https://chateaudechantilly.fr/la-foret/ensemble-sauvons-la-foret-de-chantilly/>, 2024. [Online; accessed 12-May-2024].
- [12] Mathieu Decuyper, Roberto O Chávez, Madelon Lohbeck, José A Lastra, Nandika Tsendbazar, Julia Hackländer, Martin Herold, and Tor-G Vågen. Continuous monitoring of forest change dynamics with satellite time series. *Remote Sensing of Environment*, 2022.
- [13] DINAMIS. French national facility for institutional procurement of vhr satellite imagery. <https://openspot-dinamis.data-terra.org>, 2024. [Online; accessed 12-May-2024].
- [14] Alexey Dosovitskiy, Lucas Beyer, Alexander Kolesnikov, Dirk Weissenborn, Xiaohua Zhai, Thomas Unterthiner, Mostafa Dehghani, Matthias Minderer, Georg Heigold, Sylvain Gelly, et al. An image is worth 16x16 words: Transformers for image recognition at scale. In *ICLR*, 2020.
- [15] Ralph Dubayah, James Bryan Blair, Scott Goetz, Lola Fatoyinbo, Matthew Hansen, Sean Healey, Michelle Hofton, George Hurtt, James Kellner, Scott Luthcke, et al. The global ecosystem dynamics investigation: High-resolution laser ranging of the Earth’s forests and topography. *Science of remote sensing*, 2020.
- [16] Yousef Erfanifard, Mohsen Lotfi Nasirabad, and Krzysztof Stereńczak. Assessment of Iran’s mangrove forest dynamics (1990–2020) using Landsat time series. *Remote Sensing*, 2022.
- [17] Etalab. Open licence 2.0. <https://www.etalab.gouv.fr/wp-content/uploads/2018/11/open-licence.pdf>, 2024. [Online; accessed 12-May-2024].
- [18] Fabian Ewald Fassnacht, Christoph Mager, Lars T Waser, Urša Kanjir, Jannika Schäfer, Ana Potočnik Buhvald, Elham Shafeian, Felix Schiefer, Liza Stančič, Markus Immitzer, et al. Forest practitioners’ requirements for remote sensing-based canopy height, wood-volume, tree species, and disturbance products. *Forestry: An International Journal of Forest Research*, 2024.
- [19] US National Science Foundation. Neon (national ecological observatory network). ecosystem structure (dp3.30015.001). <https://data.neonscience.org/>, 2024. Dataset accessed from <https://data.neonscience.org/data-products/DP3.30015.001> on October 11, 2024.
- [20] David LA Gaveau and Ross A Hill. Quantifying canopy height underestimation by laser pulse penetration in small-footprint airborne laser scanning data. *Canadian Journal of Remote Sensing*, 2003.

- [21] Timnit Gebru, Jamie Morgenstern, Briana Vecchione, Jennifer Wortman Vaughan, Hanna Wallach, Hal Daumé Iii, and Kate Crawford. Datasheets for datasets. *Communications of the ACM*, 2021.
- [22] Stephan Getzin, Kerstin Wiegand, and Ingo Schöning. Assessing biodiversity in forests using very high-resolution images and unmanned aerial vehicles. *Methods in ecology and evolution*, 2012.
- [23] Alan R Gillespie, Anne B Kahle, and Richard E Walker. Color enhancement of highly correlated images. ii. channel ratio and “chromaticity” transformation techniques. *Remote Sensing of Environment*, 1987.
- [24] Matthew C Hansen, Peter V Potapov, Rebecca Moore, Matt Hancher, Svetlana A Turubanova, Alexandra Tyukavina, David Thau, Stephen V Stehman, Scott J Goetz, Thomas R Loveland, and others. High-resolution global maps of 21st-century forest cover change. 2013.
- [25] Edward J Hu, Yelong Shen, Phillip Wallis, Zeyuan Allen-Zhu, Yuanzhi Li, Shean Wang, Lu Wang, and Weizhu Chen. LoRa: Low-rank adaptation of large language models. *ICLR*, 2022.
- [26] Claudia Huertas, Daniel Sabatier, Géraldine Derroire, Bruno Ferry, Toby D Jackson, Raphaël Pélissier, and Grégoire Vincent. Mapping tree mortality rate in a tropical moist forest using multi-temporal LiDAR. *International Journal of Applied Earth Observation and Geoinformation*, 2022.
- [27] IGN. Lidar hd technical description. https://geoservices.ign.fr/sites/default/files/2023-10/DC_LiDAR_HD_1-0_PTS.pdf. Online; accessed 2024-02-21.
- [28] IGN. More than 190 tree species inventoried in france. <https://inventaire-forestier.ign.fr/spip.php?article175>, 2024. [Online; accessed 12-May-2024].
- [29] IGN. LiDAR HD : Vers une nouvelle cartographie 3d du territoire. <https://www.ign.fr/institut/lidar-hd-vers-une-nouvelle-cartographie-3d-du-territoire>, 2024. [Online; accessed 12-May-2024].
- [30] IGN. Forest data base. <https://geoservices.ign.fr/bdforet>, 2024. [Online; accessed 12-May-2024].
- [31] Colbert M Jackson and Elhadi Adam. Remote sensing of selective logging in tropical forests: Current state and future directions. *iForest-Biogeosciences and Forestry*, 2020.
- [32] Ekaterina Kalinicheva, Loic Landrieu, Clément Mallet, and Nesrine Chehata. Multi-layer modeling of dense vegetation from aerial LiDAR scans. In *CVPR Workshop Earth Vision*, 2022.
- [33] Rodney J Keenan. Climate change impacts and adaptation in forest management: A review. *Annals of forest science*, 2015.
- [34] Diederik P Kingma and Jimmy Ba. Adam: A method for stochastic optimization. *ICLR*, 2015.
- [35] Tobias Kuemmerle, Oleh Chaskovskyy, Jan Knorn, Volker C Radeloff, Ivan Kruhlov, William S Keeton, and Patrick Hostert. Forest cover change and illegal logging in the Ukrainian Carpathians in the transition period from 1988 to 2007. *Remote Sensing of Environment*, 2009.
- [36] Nico Lang, Walter Jetz, Konrad Schindler, and Jan Dirk Wegner. A high-resolution canopy height model of the Earth. *Nature Ecology & Evolution*, 2023.
- [37] Stéphane Lecq, Anne Loisel, Francois Brischoux, Stephen J Mullin, and Xavier Bonnet. Importance of ground refuges for the biodiversity in agricultural hedgerows. *Ecological Indicators*, 2017.
- [38] Siyu Liu, Martin Brandt, Thomas Nord-Larsen, Jerome Chave, Florian Reiner, Nico Lang, Xiaoye Tong, Philippe Ciais, Christian Igel, Adrian Pascual, et al. The overlooked contribution of trees outside forests to tree cover and woody biomass across Europe. *Science Advances*, 2023.
- [39] Ze Liu, Yutong Lin, Yue Cao, Han Hu, Yixuan Wei, Zheng Zhang, Stephen Lin, and Baining Guo. SWIN transformer: Hierarchical vision transformer using shifted windows. In *ICCV*, 2021.
- [40] Kenneth G MacDicken. Global forest resources assessment 2015: What, why and how? *Forest Ecology and Management*, 2015.
- [41] Kenneth G MacDicken, Phosiso Sola, John E Hall, Cesar Sabogal, Martin Tadoum, and Carlos de Wasseige. Global progress toward sustainable forest management. *Forest Ecology and Management*, 2015.
- [42] Ronald E McRoberts and Erkki O Tomppo. Remote sensing support for national forest inventories. *Remote sensing of environment*, 2007.
- [43] French Ministry of Agriculture. The national forest and wood programme (PNFB). https://inis.iaea.org/search/search.aspx?orig_q=RN:51010336, 2024. [Online; accessed 12-May-2024].
- [44] United States Department of Agriculture. National agriculture imagery program (NAIP). https://www.fsa.usda.gov/Assets/USDA-FSA-Public/usdfiles/APFO/support-documents/pdfs/naip_infosheet_2016.pdf, 2024. [Online; accessed 12-May-2024].
- [45] Federal Office of Topography Swisstopo. Swisstopo orthophotos. <https://www.swisstopo.admin.ch/fr/orthophotos>, 2024. [Online; accessed 12-May-2024].

- [46] Federal Office of Topography Swisstopo. Swisstopo LiDAR data acquisition. <https://www.swisstopo.admin.ch/en/lidar-data-swisstopo>, 2024. [Online; accessed 12-May-2024].
- [47] Maxime Oquab, Timothée Darcet, Théo Moutakanni, Huy V Vo, Marc Szafraniec, Vasil Khalidov, Pierre Fernandez, Daniel HAZIZA, Francisco Massa, Alaaeldin El-Nouby, et al. DINOv2: Learning robust visual features without supervision. *TMLR*, 2023.
- [48] Jan Pauls, Max Zimmer, Una M Kelly, Martin Schwartz, Sassan Saatchi, Philippe Ciais, Sebastian Pokutta, Martin Brandt, and Fabian Gieseke. Estimating canopy height at scale. In *ICML*, 2024.
- [49] Murray C Peel, Brian L Finlayson, and Thomas A McMahon. Updated world map of the Köppen-Geiger climate classification. *Hydrology and earth system sciences*, 2007.
- [50] Guan Peng and ZHENG Yili. Research on forest phenology prediction based on LSTM and GRU model. *Journal of Resources and Ecology*, 2022.
- [51] Peter Potapov, Xinyuan Li, Andres Hernandez-Serna, Alexandra Tyukavina, Matthew C Hansen, Anil Komareddy, Amy Pickens, Svetlana Turubanova, Hao Tang, Carlos Edibaldo Silva, et al. Mapping global forest canopy height through integration of GEDI and Landsat data. *Remote Sensing of Environment*, 2021.
- [52] Hans Pretzsch, Miren Del Río, Catia Arcangeli, Kamil Bielak, Malgorzata Dudzinska, David Ian Forrester, Joachim Klädtke, Ulrich Kohnle, Thomas Ledermann, Robert Matthews, et al. Forest growth in Europe shows diverging large regional trends. *Scientific Reports*, 2023.
- [53] Jushuang Qin, Menglu Ma, Yutong Zhu, Baoguo Wu, and Xiaohui Su. 3PG-MT-LSTM: A hybrid model under biomass compatibility constraints for the prediction of long-term forest growth to support sustainable management. *Forests*, 2023.
- [54] Alec Radford, Jong Wook Kim, Chris Hallacy, Aditya Ramesh, Gabriel Goh, Sandhini Agarwal, Girish Sastry, Amanda Askell, Pamela Mishkin, Jack Clark, et al. Learning transferable visual models from natural language supervision. In *ICML*, 2021.
- [55] Colorado J Reed, Ritwik Gupta, Shufan Li, Sarah Brockman, Christopher Funk, Brian Clipp, Kurt Keutzer, Salvatore Candido, Matt Uyttendaele, and Trevor Darrell. Scale-MAE: A scale-aware masked autoencoder for multiscale geospatial representation learning. In *ICCV*, 2023.
- [56] Christopher PO Reyer, Ramiro Silveyra Gonzalez, Klara Dolos, Florian Hartig, Ylva Hauf, Matthias Noack, Petra Lasch-Born, Thomas Rötzer, Hans Pretzsch, Henning Meessenburg, et al. The PROFOUND database for evaluating vegetation models and simulating climate impacts on European forests. *Earth System Science Data*, 2020.
- [57] Tal Ridnik, Emanuel Ben-Baruch, Asaf Noy, and Lih Zelnik-Manor. ImageNet-21K pretraining for the masses. In *NeurIPS Datasets and Benchmarks Track*, 2021.
- [58] Olaf Ronneberger, Philipp Fischer, and Thomas Brox. UNet: Convolutional networks for biomedical image segmentation. In *MICCAI*. Springer, 2015.
- [59] Olga Russakovsky, Jia Deng, Hao Su, Jonathan Krause, Sanjeev Satheesh, Sean Ma, Zhiheng Huang, Andrej Karpathy, Aditya Khosla, Michael Bernstein, et al. ImageNet large scale visual recognition challenge. *IJCV*, 2015.
- [60] Anouk Schleich, Sylvie Durrieu, and Cédric Vega. Improving gedi footprint geolocation using a high resolution digital elevation model. *IEEE Journal of Selected Topics in Applied Earth Observations and Remote Sensing*, 2023.
- [61] Martin Schwartz. *Mapping forest height and biomass at high resolution in France with satellite remote sensing and deep learning*. PhD thesis, Université Paris-Saclay, 2023.
- [62] Martin Schwartz, Philippe Ciais, Aurélien De Truchis, Jérôme Chave, Catherine Ottlé, Cedric Vega, Jean-Pierre Wigneron, Manuel Nicolas, Sami Jouaber, Siyu Liu, Martin Brandt, and Ibrahim Fayad. FORMS: Forest multiple source height, wood volume, and biomass maps in France at 10 to 30m resolution based on Sentinel-1, Sentinel-2, and GEDI data with a deep learning approach. *Earth System Science Data*, 2023.
- [63] Gary S Smith. Digital orthophotography and GIS. In *Proceedings of the 1995 ESRI user conference*, 1995.
- [64] Nathan L Stephenson, AJ Das, R Condit, SE Russo, PJ Baker, Noelle G Beckman, DA Coomes, ER Lines, WK Morris, Nadja Rüger, et al. Rate of tree carbon accumulation increases continuously with tree size. *Nature*, 2014.
- [65] Hao Tang, Jason Stoker, Scott Luthcke, John Armston, Kyungtae Lee, Bryan Blair, and Michelle Hofton. Evaluating and mitigating the impact of systematic geolocation error on canopy height measurement performance of GEDI. *Remote Sensing of Environment*, 2023.
- [66] Sara T Thompson and William B Magrath. Preventing illegal logging. *Forest Policy and Economics*, 2021.
- [67] Feng Tian, Zhanzhang Cai, Hongxiao Jin, Koen Hufkens, Helfried Scheffinger, Torbern Tagesson, Bruno Smets, Roel Van Hoolst, Kasper Bonte, Eva Ivits, et al. Calibrating vegetation phenology from Sentinel-2 using eddy covariance, PhenoCam, and PEP725 networks across Europe. *Remote Sensing of Environment*, 2021.

- [68] Jamie Tolan, Hung-I Yang, Benjamin Nosarzewski, Guillaume Couairon, Huy V Vo, John Brandt, Justine Spore, Sayantan Majumdar, Daniel Haziza, Janaki Vamaraju, et al. Very high resolution canopy height maps from RGB imagery using self-supervised vision transformer and convolutional decoder trained on aerial LiDAR. *Remote Sensing of Environment*, 2024.
- [69] Erkki Tomppo, Thomas Gschwantner, Mark Lawrence, Ronald E McRoberts, Karl Gabler, K Schadauer, Claude Vidal, A Lanz, Göran Ståhl, Emil Cienciala, et al. National forest inventories. *Pathways for Common Reporting. European Science Foundation*, 2010.
- [70] Svetlana Turubanova, Peter Potapov, Matthew C Hansen, Xinyuan Li, Alexandra Tyukavina, Amy H Pickens, Andres Hernandez-Serna, Adrian Pascual Aranz, Juan Guerra-Hernandez, Cornelius Senf, et al. Tree canopy extent and height change in Europe, 2001–2021, quantified using Landsat data archive. *Remote Sensing of Environment*, 2023.
- [71] FH Wagner, S Roberts, AL Ritz, G Carter, R Dalagnol, S Favrichon, M Hirye, M Brandt, P Ciais, and S Saatchi. Sub-meter tree height mapping of California using aerial images and LiDAR-informed U-Net model. *Remote Sensing of Environment*, 2024.
- [72] Wenhai Wang, Enze Xie, Xiang Li, Deng-Ping Fan, Kaitao Song, Ding Liang, Tong Lu, Ping Luo, and Ling Shao. PVTv2: Improved baselines with pyramid vision transformer. *Computational Visual Media*, 2022.
- [73] Guo Dong Yang and Xiang Zhu. Ortho-rectification of SPOT 6 satellite images based on RPC models. *Applied Mechanics and Materials*, 2013.
- [74] Long Ye, Lei Gao, Raymundo Marcos-Martinez, Dirk Mallants, and Brett A Bryan. Projecting Australia’s forest cover dynamics and exploring influential factors using deep learning. *Environmental Modelling & Software*, 2019.
- [75] Xiaowei Yu, Juha Hyypä, Harri Kaartinen, and Matti Maltamo. Automatic detection of harvested trees and determination of forest growth using airborne laser scanning. *Remote sensing of Environment*, 2004.
- [76] Xiaowei Yu, Juha Hyypä, Antero Kukko, Matti Maltamo, and Harri Kaartinen. Change detection techniques for canopy height growth measurements using airborne laser scanner data. *Photogrammetric Engineering & Remote Sensing*, 2006.
- [77] Yanchao Zhang, Hanxuan Wu, and Wen Yang. Forests growth monitoring based on tree canopy 3D reconstruction using UAV aerial photogrammetry. *Forests*, 2019.

Open-Canopy: Towards Very High Resolution Forest Monitoring

Supplementary Material

We present additional results, analyses, and experiments to support our study. First, we detail our validation of the ground truth using terrain measurements and manual verifications in Sec. A. Next, we provide further results in Sec. B, including new analyses, qualitative illustrations, and experimental settings. We then conduct a detailed ablation study in Sec. C to examine the influence of key hyperparameters and design choices. Additionally, we offer a comprehensive description of the dataset and its construction in Sec. D. Finally, we provide the Datasheet for Dataset [21] for our benchmark.

A. Validation with Field Measurements

Ensuring the accuracy of our ground truth data is crucial for the validity of any computer vision benchmark. While the ALS data from LIDAR-HD have been calibrated and validated internally by the French Mapping Agency (IGN) using plots annotated by the National Forest Office (ONF), we performed additional manual verifications to further confirm their reliability, performed at plot-level and tree-level.

Plot-Level Assessment. We sourced measurements from 135 plots, each with a 15 m radius, across the test set of Open-Canopy. These plots were measured in the field by forestry experts from the National Forest Inventory (INF) within two years of the ALS acquisition. For each plot, we compared the height of the tallest tree measured in situ with the maximum canopy height in the plot as estimated by the ALS data and predicted by our best-performing computer vision model (PVTv2). As shown in Fig. Aa and detailed in Fig. Ab, the ALS-derived heights exhibit smaller errors compared to our model’s estimates and align closely with the field measurements. This validation confirms the suitability of the ALS data as ground truth for our open-access benchmark.

Tree-Level Assessment. We extended our validation to the individual tree level using data provided by the ONF, consisting of 44 geolocated trees in the Grand Est region. For each tree, we compared the measured height with the highest estimated or predicted height within a 1.5 m radius around the tree’s center. The metrics presented in Fig. Ac corroborate the plot-level findings, further validating the ALS-derived heights. This validation process emphasizes the reliability of our ground truth data, which is essential for advancing computer vision methods in canopy height estimation.

Change Dataset Curation. To ensure the quality and accuracy of the Open-Canopy- Δ benchmark, we conducted a thorough manual validation of the dieback areas constituting its ground truth. As detailed in Section 4.1, each of the 73 change areas was carefully examined and validated by a forest expert. This meticulous process guarantees the reliability of the dataset for challenging computer vision tasks involving canopy height change detection. An example of visual annotation from this validation process is shown in Fig. C. Some false positives were identified, likely due to selective logging activities occurring between the ALS and SPOT acquisitions within the same year.

B. Additional Results

We present several additional analyses of the performance of our models. First, we provide additional qualitative illustrations in Sec. B.1. Then, we offer a detailed analysis of how tree height influences the quality of the results Sec. B.2. Finally, we re-evaluate our models and other products at different resolutions (Sec. B.3), providing a fair comparison in settings more advantageous to coarser predictions.

B.1. Qualitative Illustrations

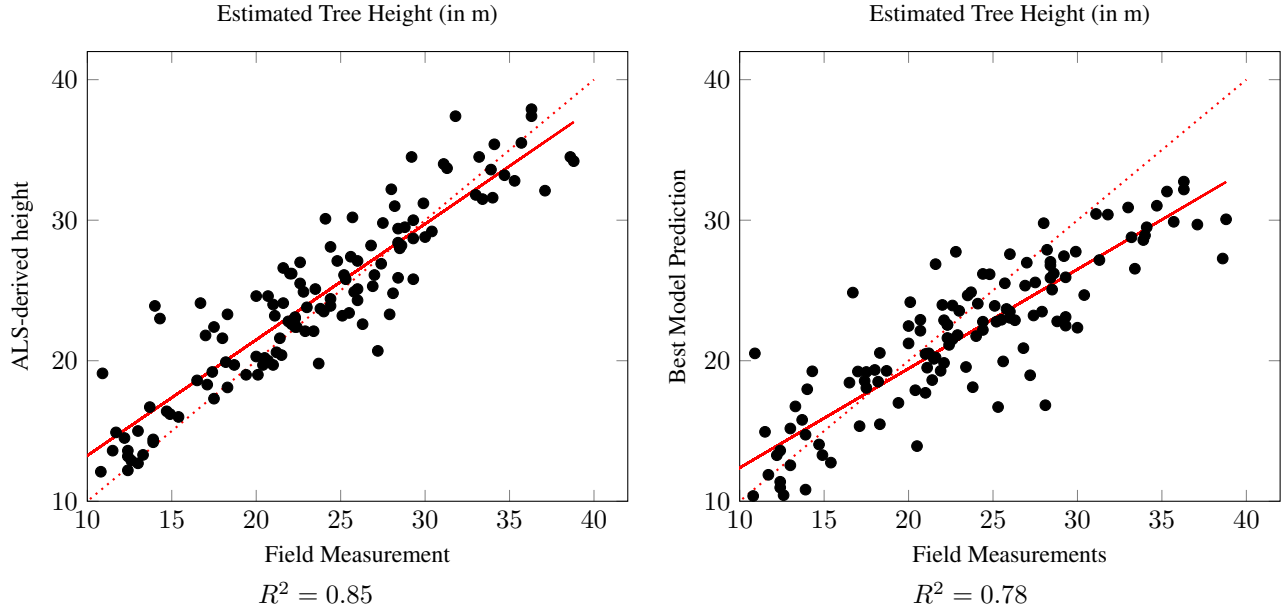
We provide here additional illustrations for qualitative assessment.

Canopy Height Fig. B showcases a comparison between the ALS-derived canopy height map and the height map predicted by our model using SPOT images. Our model demonstrates the ability to accurately estimate vegetation height across a variety of challenging scenarios:

- **Mountainous Areas** (first row): Capturing complex terrain and varied vegetation.
- **Agricultural Lands** (second row): Detecting small hedges and understory vegetation.
- **Dense Forests** (rows 3 and 4): Handling thick canopy cover and shadowed regions.
- **Urban Environments** (row 5): Distinguishing trees amidst buildings and infrastructure.
- **Mixed Scenes** (rows 6 and 7): Managing heterogeneous landscapes with multiple land cover types.

The high spatial resolution of our predictions not only captures fine-grained details but also enables the identification of man-made features such as forest paths, which are crucial for forest management applications.

We further compare the performance of three models in Fig. D: a standard Vision Transformer (ViT) and two hierarchical models, PVTv2 and SWIN. The hierarchical models



(a) **Plot-Level Scatter-Plot.** We represent the maximum heights as measured through ALS or predicted by a PVTv2 model against the manual field measurements.

(b) **Plot-Level Quantitative Evaluation.** We compare the precision of ALS and a PVTv2 model when taking the field measurements as ground truth.

	MAE (m)	nMAE (%)	RMSE (m)	Bias (m)
ALS vs Field measurements	2.3	13.5	3.1	1.2
PVTv2 vs Field measurements	2.9	14.4	3.7	-1.1

(c) **Tree-Level Quantitative Evaluation.** We compare the precision of ALS and a PVTv2 model when taking the field measurements as ground truth.

	MAE (m)	nMAE (%)	RMSE (m)	Bias (m)
ALS vs Field measurements	1.45	6.7	2.0	0.22
PVTv2 vs Field measurements	4.0	15.4	5.1	-3.2

Figure A. Field-Verification of Height Maps. We validate our ALS-based ground truth by comparing it to field measurements at two scales: plot-level and tree-level.

exhibit significantly lower errors, which corroborates our quantitative results.

Canopy Height Change We provide additional illustrations of height change detection in Fig. E. While our model tends to over predict small growth or loss of canopy height, the areas of strong disturbances—as denoted by our smoothed and filtered binary change maps—are overall well detected and delineated. Our illustration covers areas of dense forests (first row) and mixed scenes (row 2 and 3). Our method can detect disturbances such as clear and selective cuts.

Note that the Sentinel-derived height maps for 2022 and 2023 were provided by the authors of [62], as only the map for 2020 is available online.

B.2. Influence of Tree Height

We analyzed the performance of our canopy height estimation model across different ranges of true tree heights to understand how tree height influences prediction accuracy. The results are summarized in Tab. A.

- Note that the nMAE (normalized Mean Absolute Error) is computed for all ranges as the average of the pixel-wise normalized absolute error:

$$\text{nMAE} = \frac{|(z_{\text{true}} - z_{\text{pred}})|}{1 + z_{\text{true}}}, \quad (\text{A})$$

where z_{true} and z_{pred} are respectively the ALS-derived and predicted height for a given pixel. The additional 1 term in the denominator makes this measure more robust for pixels corresponding to low vegetation.

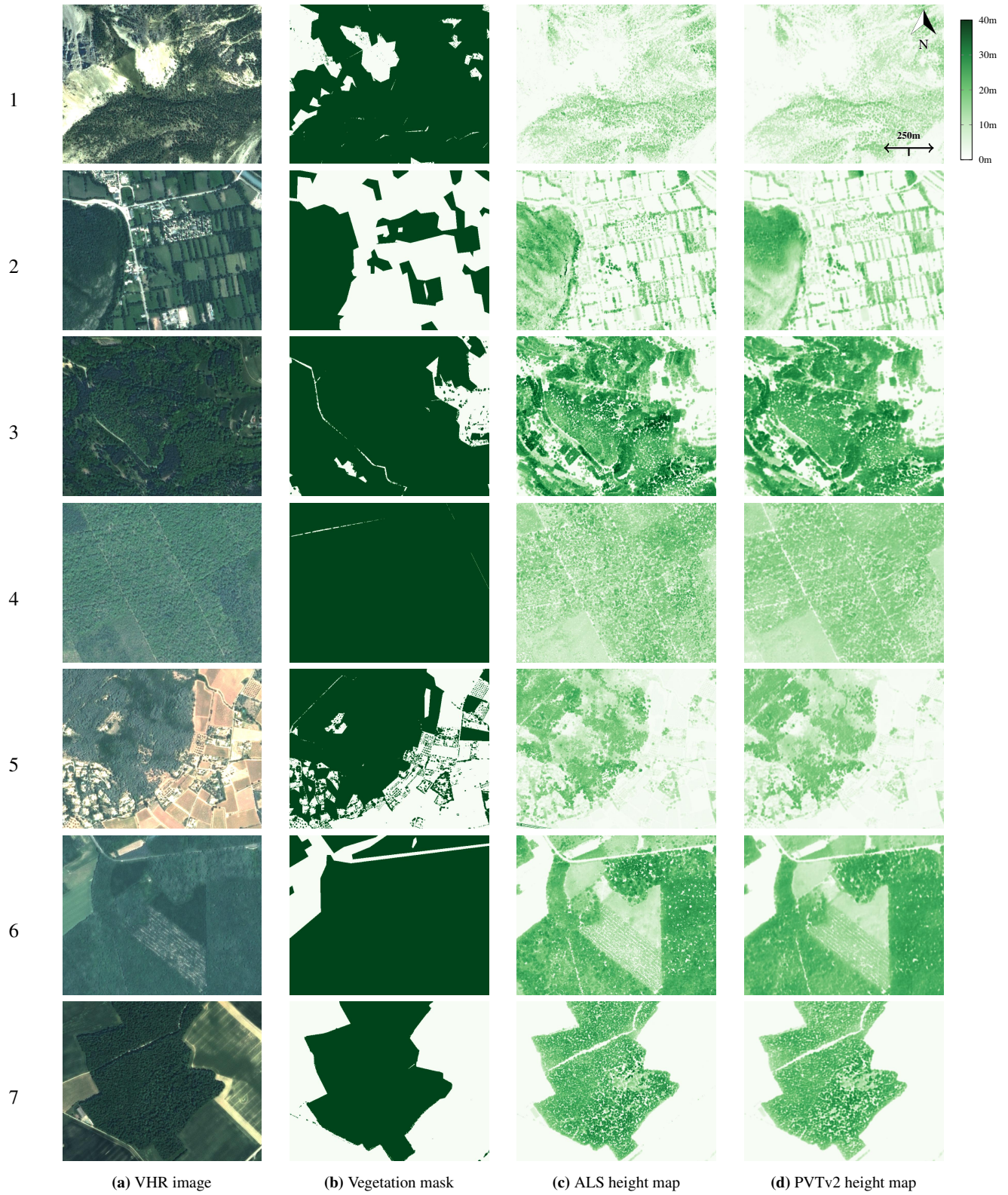


Figure B. Canopy Height Estimation Illustrations. We select seven areas of interest and represent the available VHR image ((a)), the vegetation mask used for evaluation ((b)), the ground truth ALS-derived height map ((c)), and the height map estimated with PVTv2 model from the VHR image ((d)). Scale and orientation are shared across all subfigures.

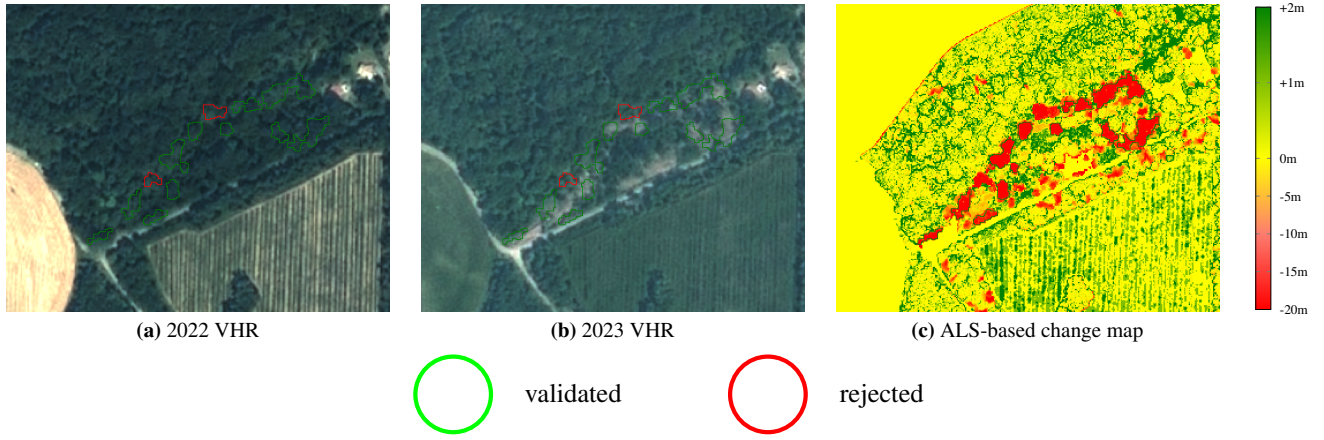


Figure C. Visual Validation of Change Components: Example of a pair of successive VHR images and the corresponding change maps (derived from differences in ALS-based canopy height). We highlight the contours of the change masks validated by forestry experts through visual inspection.

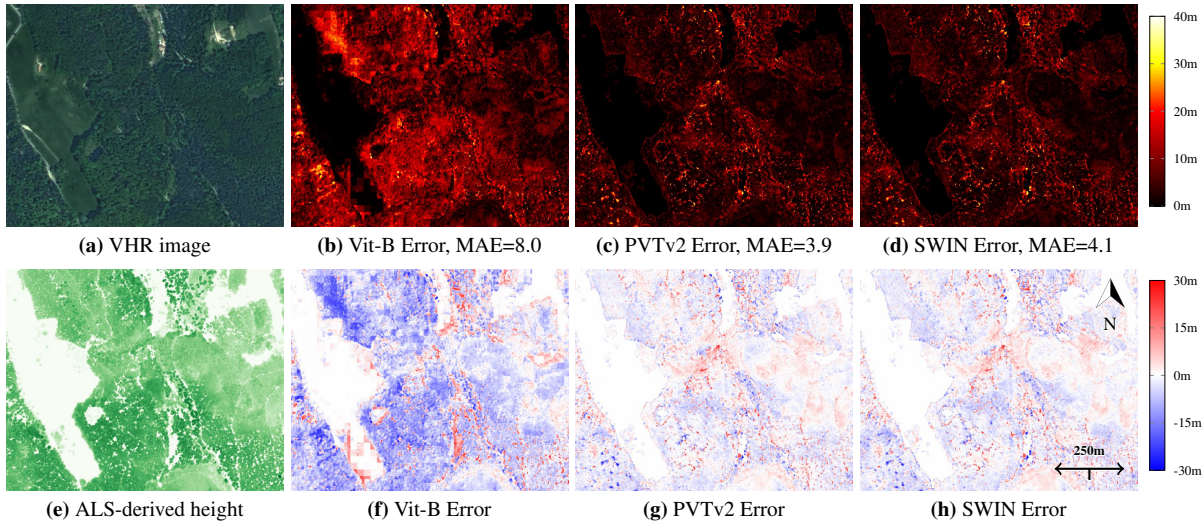


Figure D. Difference Maps: Per-pixel absolute (top row) and relative (bottom row) errors for three models: ViT-B, PVTv2, and SWIN. While the differences between PVTv2 and SWIN are subtle (approximately 20cm on average), the advantage of these models over ViT-B is visible.

- When computing the nMAE for the overall range of 0–60 m, we exclude the 0–2 m bin. This exclusion is necessary because values in this range can produce disproportionately large errors due to the normalization, which can dominate the metric and skew the results. Additionally, including this bin may unfairly disadvantage models with lower spatial resolutions that aim to predict the highest value within larger pixels, potentially overlapping with bare soil at higher resolutions.

As shown in Tab. A by the bias of our model for different ranges, our model tends to over-predict the height of small trees and under-predict the height of tall trees. While the average error is higher for larger trees, our model has the lowest nMAE for the 20–30m range, with a value of 12.1%.

B.3. Evaluation at a resolution of 10m

To provide a fair comparison with models predicting canopy height at a 10 m resolution, we resampled both our ground truth and predicted height maps to a 10 m grid and re-evaluated all available models. We performed this by aggregating the higher-resolution data as follows:

For each 10 m pixel, we took the maximum value from the overlapping 1.5 m pixels. This approach is equivalent to rasterizing the full ALS 3D point cloud directly onto a 10 m grid. Taking the maximum value aligns with models trained to predict metrics like GEDI RH100 or RH95 (relative height at the 100th or 95th percentile), which represent the tallest canopy elements within a pixel.

We report the results in Tab. B, and observe a similar ordering than in Table 3 of the main paper. All methods see improved metrics as the problem is simpler, except for Tolan *et al.* In

Table A. Canopy Height Prediction Per Height Bins. We report the metrics for different bins of true tree height for the PVTv2[72] model.

Range in m	0-2	2-5	5-10	10-15	15-20	20-30	30-60	0-60
MAE in m	1.67	2.29	2.65	2.70	2.61	3.00	5.52	2.52
nMAE in %	138.8	53.6	32.1	20.3	14.3	12.1	16.0	22.9
RMSE in m	4.31	3.67	3.69	3.60	3.53	4.19	7.56	4.02
Bias in m	1.49	0.87	0.65	0.21	-0.42	-1.90	-5.31	0.00
Tree cov. IoU (%)	-	72.6	96.5	99.3	99.7	99.8	99.6	90.5

Table B. Canopy Height Prediction at 10m resolution. We resample all ground truth and predicted maps on a 10 m grid.

Map	Backbone	Initial res. in m	MAE in m	nMAE in %	RMSE in m	Bias in m	Tree cov. IoU in %
Potapov [51]	UNet	30	6.17	44.6	8.33	-3.31	80.2
Schwartz [61, 62]	UNet	10	4.00	26.9	5.28	-1.38	90.1
Lang [36]	CNN	10	8.64	92.9	29.25	6.27	90.1
Pauls [48]	UNet	10	4.59	32.9	5.96	0.34	90.1
Liu [38]	UNet	3.0	4.58	37.4	10.97	-1.26	88.2
Tolan [68]	ViT-L	1.0	6.10	42.1	7.95	-5.37	81.6
Open-Canopy	UNet	1.5	2.72	19.0	3.95	-2.06	93.4
Open-Canopy	PVTv2	1.5	2.42	17.6	3.57	-1.69	93.3

particular, the tree coverage problem becomes significantly easier at this resolution, with all 10 m-resolution methods nearing 90% IoU. Note that the height map of [38] at a resolution of 3m was provided directly by the authors and is not available online.

C. Ablation Study

We propose an analysis of the influence of several of our hyperparameters and design choices.

C.1. Parameters of the Change Detection

We evaluate how different configurations of the ground truth binary change map affect canopy height change detection. Specifically, we examine: (i) Minimum Height Difference: The threshold for considering a pixel as having a significant change in canopy height; (ii) Minimum Contiguous Change Area: The smallest area of connected changed pixels considered significant.

Tab. C presents the IoU metrics for various combinations of these parameters. Naturally, focusing on larger change areas simplifies the detection problem due to reduced complexity. The influence of the minimum tree height change threshold is less straightforward; higher thresholds require precise detection of significant height reductions, which can be more challenging. Our chosen parameters—15 m minimum height difference and 200 m² minimum change area—represent changes that are visually detectable between images (see Fig. E), providing a realistic yet challenging task for com-

puter vision models. 01

C.2. Impact of Initialization Strategy

We provide in Tab. D the results of ablation experiments. We evaluate the impact of omitting the near infrared (NIR) band from input images. We can see in Tab. D that removing the NIR channel from input images decreases the performance for both UNet and PVTv2 backbones. Moreover, we assess various initialization strategies for fine-tuning networks initially trained only on RGB data to accommodate an additional NIR channel. Those include training from scratch, randomizing the first layer, and using LoRa. In Fig. F we show the results for different LoRa ranks and show only the best rank (32) in Tab. D. We see a clear benefit in using our proposed initialization scheme.

D. Dataset description

We describe here in details the dataset used in Open-Canopy and provide information about its constitution.

D.1. Access

- The dataset and model weights are hosted at [URL] with download and usage instructions at [URL].
- The data is governed by the Open License 2.0 of Etalab (<https://www.etalab.gouv.fr/wp-content/uploads/2018/11/open-licence.pdf>).

Table C. Canopy Height Change Detection We compute the IoU metric (in %) for various minimum height difference (row, in m) and minimum contiguous area of change (column, in m²). The values chosen in the benchmark are underlined.

min diff \ min surf	10 m ²	25 m ²	100 m ²	<u>200 m²</u>	300 m ²	400 m ²
	-5 m	7.0	7.1	7.2	6.2	5.2
-10 m	17.1	17.9	22.6	23.6	25.1	28.7
<u>-15 m</u>	22.1	23.4	28.8	37.0	40.6	40.8
-20 m	18.9	20.2	31.4	36.6	31.8	31.5

Table D. Ablation Study. We evaluate the impact of omitting the NIR channel from input images and assess various initialization strategies for fine-tuning networks initially trained only on RGB data to accommodate an additional NIR channel.

			MAE (m)	nMAE (%)	RMSE (m)	Bias (m)
Channels	backbone	pretraining				
RGB	UNet	ImageNet1K	2.77	24.8	4.34	-0.17
RGB+IR	UNet	ImageNet1K	2.67	23.8	4.18	-0.30
RGB	PVTv2	ImageNet1K	3.73	32.6	5.53	-0.50
RGB+IR	PVTv2	ImageNet1K	2.52	22.9	4.02	0.00
Initialization	backbone	pretraining				
Fully random			11.17	85.77	14.38	-10.94
Rand. 1st layer			2.87	24.3	4.24	-0.04
LoRA (rank 32)	PVTv2	ImageNet1K	3.64	32.8	5.40	-0.27
Proposed			2.52	22.9	4.02	0.00

- Codes for data preprocessing, training models and evaluation are available at [URL].

D.2. Composition

We describe here the organization of the dataset. See Section E for details on how the dataset was prepared.

The dataset is organized in the following way:

- The folder `canopy_height` contains data for canopy height estimation.
- The folder `canopy_height_change` contains data for canopy height change estimation.

The composition of the `canopy_height` folder is the following:

- The file `geometries.geojson` stores a list of 95,429 1km² square geolocated geometries, giving access to the splits of the dataset. It can be loaded using the python package `geopandas`¹. Each geometry designates either a train, validation, test or buffer area. This information is stored in the column `split`. There are 8,046 buffer tiles, 66,339 train tiles, 7,369 validation tiles and 13,675 test tiles. Additionally, each geometry is associated to a year (corresponding to the year of

the corresponding LiDAR acquisition), stored in the column `lidar_year`.

- The file `forest_mask.parquet` stores geolocated geometries of forests' outlines. It can be loaded using the python package `geopandas`. The parquet format is used to accelerate loading time.
- Each folder 2021, 2022 and 2023 contains three files:
 - `spot.vrt` is a geolocated virtual file that gives access to SPOT 6-7 images stored in the subfolder `spot`. It can be accessed through Qgis software² or python `rasterio` library³ for instance. It has the same extent as the geometries of the associated year.
 - Similarly `lidar.vrt` gives access to ALS-derived (LiDAR) canopy height maps stored in the subfolder `lidar`.
 - Similarly `lidar_classification.vrt` gives access to classification rasters stored in the subfolder `lidar_classification`.

The composition of the `canopy_height_change` folder is the following:

¹ <https://geopandas.org/en/stable/>

² <https://www.qgis.org/en/site/>

³ <https://rasterio.readthedocs.io/en/stable/>

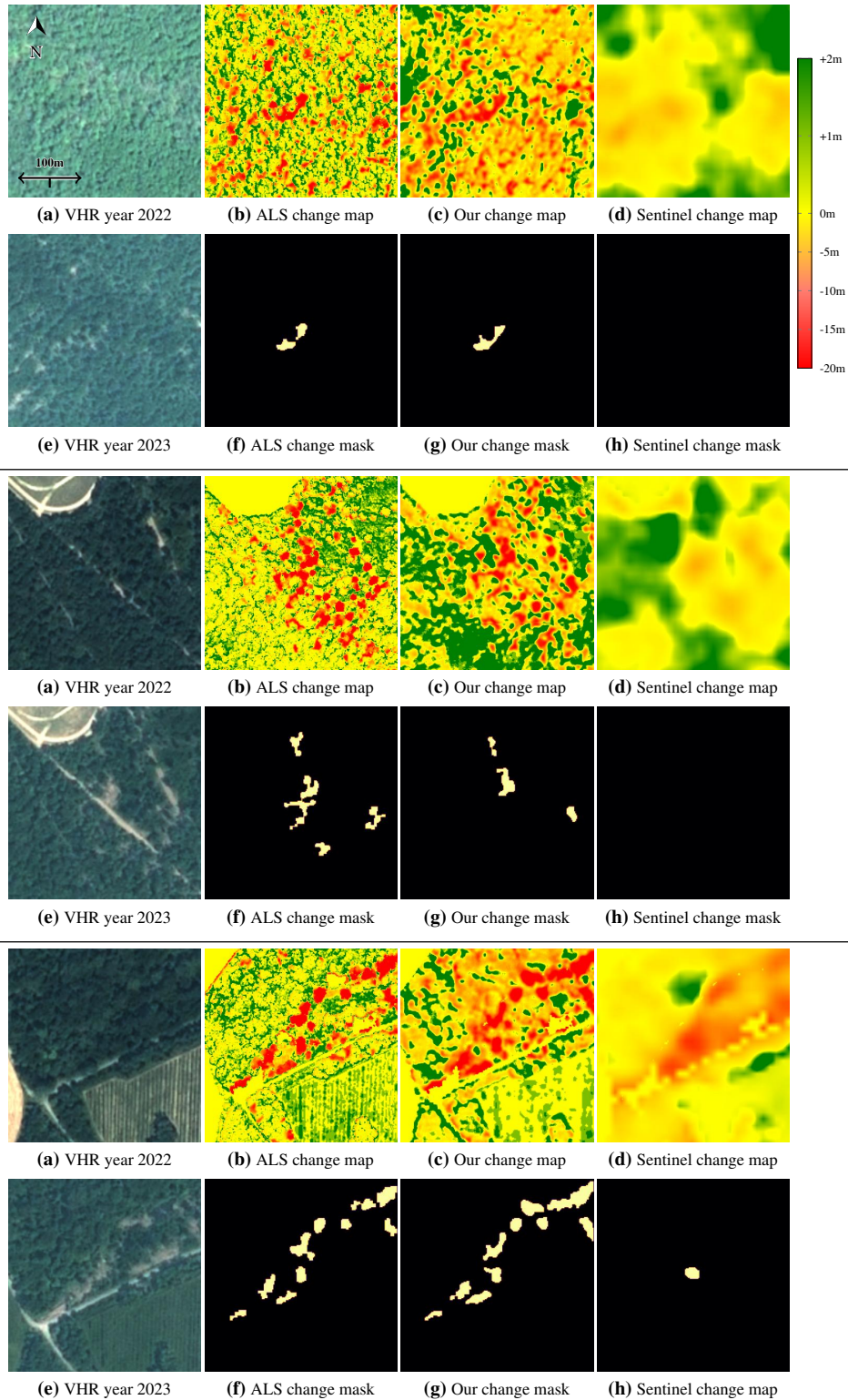


Figure E. Canopy Height Change. We consider VHR images taken in 2022 and 2023 in Chantilly Forest: (a) and (e), and use ALS observations of the same years to derive a canopy height change map (b). We compare this map to the ones predicted by a PVTv2 model (c) and by a model from Schwartz *et al.* trained on Sentinel data [62]. We also compare the binary change masks derived from ALS measurements (f) and from predicted change maps: (g) and (h). Scale and orientation are shared across all subfigures.

- The file `spot_1.tif` is a geolocalized image extracted from SPOT 6-7 images in the year 2022 in the area of Chantilly, France.
- The file `spot_2.tif` is a geolocalized image extracted from SPOT 6-7 images in the year 2023 in the area of Chantilly (France).
- The file `lidar_1.tif` is a geolocalized ALS-derived height map in the year 2022 in the area of Chantilly (France), derived from LiDAR HD [29].
- The file `lidar_2_m.tif` is a geolocalized ALS-derived height map in the year 2023 in the area of Chantilly (France), provided by [11], at a resolution of 1m, with height in meters, and covering only forests.
- The file `predictions_1_m.tif` is a geolocalized height map predicted by a PVTv2 model in 2022 in the area of Chantilly (France), in meter unit.
- The file `predictions_2_m.tif` is a geolocalized height map predicted by a PVTv2 model in 2023 in the area of Chantilly (France), in meter unit.
- The file `lidar_classification.tif` is an ALS-derived classification raster in 2022 in the area of Chantilly (France).
- Additionally, files that follow the following pattern `*_masked.tif` designate images masked on the extent of the available ALS data for 2023.
- The file `change_mask_delta_15_surface_200_annotated.geojson` can be loaded with `geopandas` and gives access to geometries detected as "change" for a minimum height difference of 15m and a minimum surface of 200m. We also provide manual annotations of detections in the column "Rating", where "true" indicates a true positive and "false" a false positive.

D.3. Characteristics

- We provide SPOT 6-7 images, ALS-derived height maps and classification rasters covering 95,429 km² (including a "buffer" area of 8046 km², a train area of 66,339 km², a validation area of 7,369 km² and a test area of 13,675 km²). Each image has a resolution of 1.5m, with one annotation per pixel, for a total of 42,455,312,381 annotations.
- Additionally, we provide SPOT 6-7 imagery, ALS-derived height maps and a classification raster on the Chantilly forest area for 2022 and 2023 (166 km²).
- The Open-Canopy dataset is derived from a larger dataset of SPOT 6-7 acquisitions across the full metropolitan French territory between 2013 and 2023⁴, and a larger dataset of ALS acquisitions from the IGN campaign that started in 2021 and aims at covering the full metropolitan French territory (LiDAR HD)⁵. The

⁴ <https://openspot-dinamis.data-terra.org>

⁵ <https://geoservices.ign.fr/lidarhd>

Open-Canopy dataset focuses on domains that are representative of the diversity of French forests and where LiDAR HD is available at the time of writing, with the goal of limiting the dataset's size to approximately 300 GB, in order to facilitate its usage by the machine learning community.

- Each SPOT image is at a resolution of 1.5 m per pixel, and features 4 spectral channels: red, blue, green, and near-infrared.
- Each height map image is at a resolution of 1.5 m per pixel, and features 1 channel (height in decimeters except if notified in the filename in the following format: "`<name>_<unit>.tif`").
- Each classification image is at a resolution of 1.5 m per pixel, and features 1 channel (classification [27] for a description of classes). Forests' outlines are stored as geometries in a parquet file. A Python utility is provided to create a vegetation mask from the classification raster and the forests' outlines.

E. Dataset preparation

E.1. Splits

Our sampling strategy is semi-automated and proceeds as follows:

- SPOT images were associated to LiDAR height maps of the same year and geolocation (each LiDAR height map corresponds to a 1km² geolocalized square tile, referred to as "geometry" in the following).
- Geometries on overlapping areas between spot full images were removed.
- Geometries that had more than 100 zeros on the first spot band (*e.g.*, on edges of a full spot image) were discarded to avoid tiles with missing data.
- Test geometries of 1km² were sampled (with a fixed seed) to form contiguous squares of 7km² and to cover 20,000 km².
- Test geometries that overlapped each other were dropped.
- Test geometries that covered different years in terms of LiDAR acquisitions were dropped.
- This process resulted in a total test area of 13,675 km².
- A buffer of 1km was applied around each test area of 7km².
- Validation and train geometries were randomly sampled (with a fixed seed) among the remaining geometries, with a proportion of 10% for validation and 90% for training.
- This process resulted in a training area of 66,339 km² and a validation area of 7,369 km².

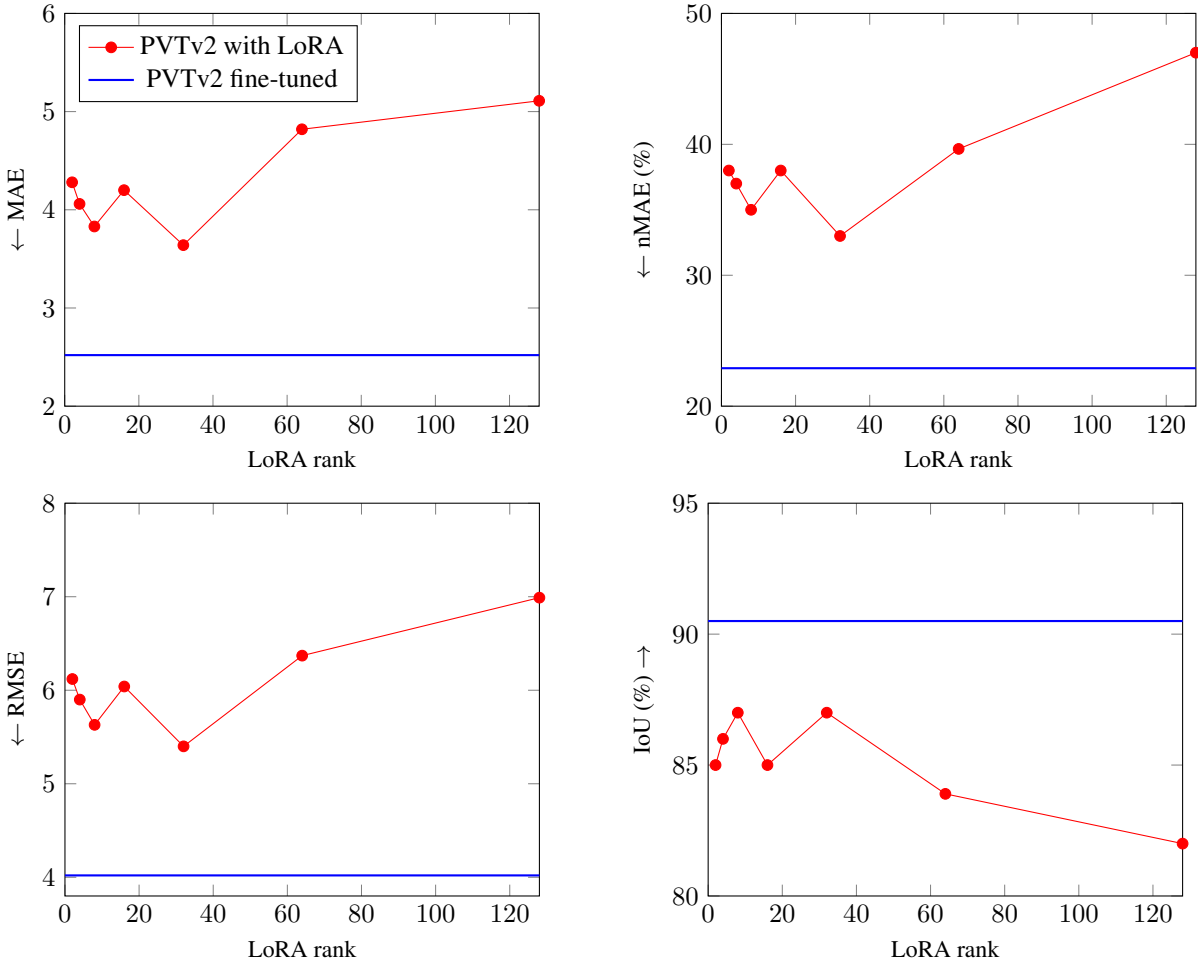


Figure F. LoRa Fine-Tuning of PVTv2. We fine-tun PVTv2 using LoRa for different rank. To allow the network to adapt to the NIR modality, we still train the first layer fully. The best results, obtained with rank = 32, are noticeably inferior to a fully fine-tunned PVTv2

E.2. SPOT 6-7 satellite imagery

- The aerial images are sampled from the DINAMIS⁶ collection. This collection consists of an annual mosaic of selected tiles taken by SPOT 6-7 satellites between March and October of each year between 2013 and 2023, covering the entire French metropolitan territory. All images are orthorectified by IGN and mapped onto a unified cartographic coordinate reference system (Lambert 93). Each tile consists of an image with four spectral bands: red, green, blue, and near-infrared at a resolution of 6m, and an image with one panchromatic band at a resolution of 1.5m that can be downloaded separately.
- A total of 52 pairs of spectral and panchromatic images were downloaded from the DINAMIS website, for each year from 2021 to 2023, to cover

- a very diverse range of forest types in areas where LiDAR HD was available at the time of the creation of the dataset.
- We applied pansharpening with the weighted Brovey algorithm [23] to upsample all four spectral bands to a resolution of 1.5m, resulting in one image with four bands for each tile.
- We cropped each image to the area covered by the ALS acquisitions of the same year.
- Pixels values were clipped to a maximum value of 2000 to avoid outliers (upper bound both quantitatively and qualitatively assessed through histograms and visualization).
- Resulting images were normalized to a 0-255 range and saved as uint8 in a block-tiled compressed tiff format (256 × 256).
- The pansharpening and normalization procedures were voluntarily kept relatively simple in order to

⁶ <https://openspot-dinamis.data-terra.org>

facilitate reproducibility. They may not be optimal for visualization, *e.g.*, lacking harmonization, but we expect deep learning models to be robust to such variations in input data.

E.3. ALS data

- The ALS classified point clouds were downloaded from the **LiDAR HD** website (IGN). A reference to each download link is saved in the file `geometries.geojson`.
- For each geometry, canopy height images were derived from ALS data by taking the maximum difference between the height of each point and the one of its nearest point classified as ground within its pixel, interpolating values in areas without data.
- LiDAR point clouds were classified by IGN into the main types of land cover (water, ground, high vegetation over 1.5m, buildings...). We use this classification to produce classification rasters at a resolution of 1.5m, where each pixel takes the value of the most frequent class of the corresponding LiDAR points.
- We then create vegetation masks by taking the union of the ALS-derived mask indicating vegetation over 1.5m in height, with the official forest plots outlines (file `forest_mask.parquet`), both provided by IGN. The resulting vegetation masks cover trees and shrubs within forest plots as well as outside, such as hedges and urban trees.
- The official forests’ outlines were extracted from “BD foret”⁷ and “simplified” using geopandas python library to a precision of 10m, with the goal to limit their size.

F. Datasheet for Open-Canopy dataset

F.1. Motivation

- **For what purpose was the dataset created?** Was there a specific task in mind? Was there a particular gap that needed to be filled? Please provide a description.
The Open-Canopy dataset was created to train and evaluate models that (i) predict very-high resolution canopy height maps from satellite imagery using LiDAR scans for ground truth, and (ii) detect canopy height changes between images from different years. The main gap we are addressing is the lack of curated open-source datasets with both very high resolution imagery and ALS-based (LiDAR) canopy height maps.
- **Who created the dataset (e.g., which team, research group) and on behalf of which entity (e.g., company, institution, organization)?** This dataset was curated

⁷ <https://geoservices.ign.fr/bdforet#telechargementv2>

by a team of researchers from ENS Paris (Ecole Normale Supérieure), LSCE (Laboratoire des Sciences du Climat et de l’Environnement), ENPC (Ecole des Ponts ParisTech), and IGN (the French National Institute of Geographical and Forest Information), using data made available by **DINAMIS** and IGN. DINAMIS [13] is a French platform that provides access to earth observation products for public benefit programs. The IGN is a French public state administrative establishment aiming to produce and maintain geographical information for France.

- **Who funded the creation of the dataset?** If there is an associated grant, please provide the name of the grantor and the grant name and number.
The funding of the Open-Canopy dataset is 100% public. Open-Canopy benefited from funding by the French National Research Agency (grant **ANR-22-FA11-0002**).
- **Any other comments?**
N/A.

F.2. Composition

- **What do the instances that comprise the dataset represent (e.g., documents, photos, people, countries)?**
The dataset is split into square areas of width 1.0005 km, rasterized to a 1.5 m resolution (667 × 667 pixels). Each instance corresponds to an area of 1 km² on the French metropolitan territory.
- **How many instances are there in total (of each type, if appropriate)?**
We provide 95,429 instances of 1km²: 66,339 train tiles, 7,369 validation tiles, 13,675 test tiles, and 8,046 “buffer” tiles. This corresponds to a total of 42,455,312,381 individual annotated pixels.
- **Does the dataset contain all possible instances or is it a sample (not necessarily random) of instances from a larger set?**
The Open-Canopy dataset covers 17% of the French metropolitan territory. It is derived from a larger dataset of SPOT 6-7 acquisitions across the full metropolitan French territory between 2013 and 2023 (<https://openspot-dinamis.data-terra.org>), and a larger dataset of ALS acquisitions from the campaign that started in 2021 and aims at covering the full metropolitan French territory (**LiDAR HD**)[29]. The Open-Canopy dataset focuses on domains that are representative of the diversity of French forests and where LiDAR HD is available at the time of submission. We also aimed to limit the dataset’s size to 300 GB to facilitate its use.
- **What data does each instance consist of?**
Each instance consists of a GeoJSON geometry (1km²), for which a 667 × 667 SPOT image, a height map, and a vegetation mask can be extracted from associated .vrt

files, in order to associate to each pixel the following values: (i) RGB and near Infrared channels derived from pan-sharpened and ortho-rectified satellite images from SPOT 6-7 acquired between 2021 and 2023; (ii) canopy height derived from LiDAR HD’s 3D point clouds [29] acquired in the same year; (iii) label (*e.g.*, vegetation, ground, water, building) derived from LiDAR HD’s 3D point clouds [29].

Additionally, we provide forest outlines obtained from IGN’s portal [30] stored as a parquet file.

- **Is there a label or target associated with each instance?**

Yes. We provide a complete pixel-precise height map and classification raster of the same extent as the satellite images.

- **Is any information missing from individual instances?**

No. We provide dense information (radiometry, canopy height, class label) for all pixels with the exception of areas that have been selected by the French government as “sensitive” for security reasons (*e.g.*, nuclear plants, military area). We do not provide the 3D point clouds from LiDAR HD, but they are accessible on their platform.

- **Are relationships between individual instances made explicit (*e.g.*, users’ movie ratings, social network links)?**

N/A.

- **Are there recommended data splits (*e.g.*, training, development/validation, testing)?**

Yes, we provide data splits for reproducing the results of the benchmark. The test split has been explicitly selected to address the complex domain shifts of geospatial data and separated from the train and validation splits by a 1 km² buffer to avoid data contamination.

- **Are there any errors, sources of noise, or redundancies in the dataset?**

The annotations from ALS (LiDAR) data include inherent inaccuracies due to the nature of the acquisition process. Multipath effects from multiple echoes can introduce errors, and outlier points may impact the quality of the canopy height maps. Additionally, variations in tree height due to different acquisition times across seasons can affect consistency between ALS and VHR acquisitions, as trees might be at various stages of their growth cycle. Input images sourced from satellite data pre-processed by IGN and DINAMIS may still exhibit artifacts due to cloud cover or contain small registration errors that can impact the analysis.

Classification rasters derived from ALS data are also subject to inaccuracies. These can stem from inherent limitations in the ALS technology, including noise in the data which may lead to errors in vegetation classifi-

cation.

- **Is the dataset self-contained, or does it link to or otherwise rely on external resources (*e.g.*, websites, tweets, other datasets)?** This dataset is self-contained and will be stored on the [Huggingface](#) platform. The dataset is under the Open License 2.0 of Etalab.

- **Does the dataset contain data that might be considered confidential (*e.g.*, data that is protected by legal privilege or by doctor–patient confidentiality, data that includes the content of individuals’ non-public communications)?**

No. The classification raster does not contain any information that would not be available in other open-access sources (DINAMIS, BD-Foret, LiDAR-HD). We have specifically avoided high-risk areas such as military installations or nuclear plants.

- **Does the dataset contain data that, if viewed directly, might be offensive, insulting, threatening, or might otherwise cause anxiety? *If so, please describe why.***

No.

- **Does the dataset identify any subpopulations (*e.g.*, by age, gender)?**

No.

- **Is it possible to identify individuals (*i.e.*, one or more natural persons), either directly or indirectly (*i.e.*, in combination with other data) from the dataset?**

No. The resolution of 1.5m per pixel and the aerial perspective makes identifying individuals impossible.

- **Does the dataset contain data that might be considered sensitive in any way (*e.g.*, data that reveals racial or ethnic origins, sexual orientations, religious beliefs, political opinions or union memberships, or locations; financial or health data; biometric or genetic data; forms of government identification, such as social security numbers; criminal history)?**

No.

- **Any other comments?**

No.

E.3. Collection Process

- **How was the data associated with each instance acquired?**

The satellite images are sampled from the DINAMIS [open SPOT](#) collection. This collection consists of an annual mosaic of selected images taken by SPOT 6-7 satellites between March and October of each year between 2013 and 2023, covering the entire French metropolitan territory. All images are preprocessed by IGN and mapped onto a unified cartographic coordinate reference system (Lambert 93).

- The ALS classified point clouds were downloaded from the [LiDAR HD](#) website (IGN).

- **What mechanisms or procedures were used to collect**

the data (e.g., hardware apparatus or sensor, manual human curation, software program, software API)? The IGN selected several acquisition companies through a call for tender with strict specifications.

- **If the dataset is a sample from a larger set, what was the sampling strategy (e.g., deterministic, probabilistic with specific sampling probabilities)?**

The sampling strategy was semi-automated. First a manual selection of spot images was manually chosen and downloaded from DINAMIS website, so as to cover a diverse range of forests types in areas where LiDAR HD was also available. Then training, validation, and test splits were randomly sampled, with constraints such as test tiles having a size of 7 km^2 and being separated from other tiles by a buffer of 1 km^2 , and covering an area of about $14,000 \text{ km}^2$. See Section E.1 for more details.

- **Who was involved in the data collection process (e.g., students, crowdworkers, contractors) and how were they compensated (e.g., how much were crowdworkers paid)?**

The data collection process for the dataset was managed by the European Space Agency (ESA), which provided the Very High Resolution (VHR) Imagery, and the French Mapping Agency (IGN), which provided the LiDAR HD data. The curation of this dataset was overseen by two individuals who were associated with academic institutions as a postdoctoral researcher (ENS) and an intern (LSCE) during the dataset's creation.

- **Over what timeframe was the data collected? Does this timeframe match the creation timeframe of the data associated with the instances (e.g., recent crawl of old news articles)?**

The collection of satellite imagery and ALS data spans from 2021 to 2023, which coincides with the period of availability of LiDAR HD data at the time of the creation of the dataset.

- **Were any ethical review processes conducted (e.g., by an institutional review board)?**

No.

- **Does the dataset relate to people?**

No.

- **Did you collect the data from the individuals in question directly, or obtain it via third parties or other sources (e.g., websites)?**

N/A.

- **Were the individuals in question notified about the data collection?**

N/A.

- **Did the individuals in question consent to the collection and use of their data?**

N/A.

- **If consent was obtained, were the consenting individuals provided with a mechanism to revoke their consent in the future or for certain uses?**

N/A.

- **Has an analysis of the potential impact of the dataset and its use on data subjects (e.g., a data protection impact analysis) been conducted?**

No. Given the nature of the dataset—which involves high-resolution canopy height data that does not include personal identifiers or directly impact individual privacy—it is unlikely that the dataset poses significant risks to data subjects. The focus is primarily on environmental features rather than personal data.

- **Any other comments?**

No.

E.4. Preprocessing, Cleaning, and/or Labeling

- **Was any preprocessing/cleaning/labeling of the data done (e.g., discretization or bucketing, tokenization, part-of-speech tagging, SIFT feature extraction, removal of instances, processing of missing values)?**

Canopy Height Maps were derived from ALS data by taking the maximum difference between the height of each point and the one of its nearest point classified as ground within its pixel, interpolating values in areas without data.

- For vegetation masks, we take the union of the ALS-derived mask indicating vegetation over 1.5m in height, with the official forest plots outlines, both provided by IGN. The resulting vegetation mask covers trees and shrubs within forest plots as well as outside, such as hedges and urban trees. The official forests' outlines were "simplified" using geopandas python library to a precision of 10m, in order to limit their size.

- SPOT 6-7 images were pansharpened with the weighted Brovey algorithm to upsample all four spectral bands to a resolution of 1.5m. Then all pixels values were clipped to a maximum value of 2000 to avoid outliers and normalized to a 0-255 range to be saved as uint8, in a block-tiled compressed tiff format.

- **Was the "raw" data saved in addition to the preprocessed/cleaned/labeled data (e.g., to support unanticipated future uses)?** *If so, please provide a link or other access point to the "raw" data.*

Yes. The raw data can be downloaded from [DINAMIS](#) and [LiDAR HD](#) websites.

- **Is the software used to preprocess/clean/label the instances available?**

Yes. All the codes to preprocess the data are available on the Github of the project <https://github.com/fajwel/Open-Canopy>.

- **Any other comments?**

No.

F.5. Uses

- **Has the dataset been used for any tasks already?**
No.
- **What (other) tasks could the dataset be used for?**
We encourage future researchers to use the Open-Canopy dataset for several tasks. Particularly, the dataset could be used to predict land cover in addition to canopy height, using the classification rasters as complimentary labels. It could also be used for pre-training of models for other tasks such as tree cover segmentation and tree species classification.
- **Is there anything about the composition of the dataset or the way it was collected and preprocessed/cleaned/labeled that might impact future uses?**
This dataset is geographically limited to metropolitan France. Although France's territory is diverse, featuring oceanic, continental, Mediterranean, and mountainous bioclimatic regions, it does not contain tropical or desert areas.
- The Open-Canopy dataset's reliance on purely optical data may limit the applicability of the models trained on it to regions with pervasive cloud cover.
- **Are there tasks for which the dataset should not be used?**
No.
- **Any other comments?**
No.

F.6. Distribution

- **Will the dataset be distributed to third parties outside of the entity (e.g., company, institution, organization) on behalf of which the dataset was created?**
Yes. the dataset will be open-source.
- **How will the dataset be distributed (e.g., tarball on website, API, GitHub)?**
The data will be hosted on Huggingface platform (<https://huggingface.co/datasets/fajwel/Open-Canopy>), with download and usage instructions on the Open-Canopy project page hosted on GitHub (<https://github.com/fajwel/Open-Canopy>).
- **When will the dataset be distributed?**
All data is already released under an open-source license, see below.
- **Will the dataset be distributed under a copyright or other intellectual property (IP) license, and/or under applicable terms of use (ToU)? If so, please describe this license and/or ToU, and provide a link or other access point to, or otherwise reproduce, any relevant licensing terms or ToU, as well as any fees associated with these restrictions.**
Yes. The data is governed by the Open Licence

2.0 of Etalab (<https://www.etalab.gouv.fr/wp-content/uploads/2018/11/open-licence.pdf>).

- **Have any third parties imposed IP-based or other restrictions on the data associated with the instances?**
No.
- **Do any export controls or other regulatory restrictions apply to the dataset or to individual instances?**
No.
- **Any other comments?**
No.

F.7. Maintenance

- **Who will be supporting/hosting/maintaining the dataset?**
Huggingface will support hosting of the dataset and metadata. LSCE will support maintenance of the dataset in case of revisions.
- **How can the owner/curator/manager of the dataset be contacted (e.g., email address)?**
fajwel.fogel@ens.fr and loic.landrieu@enpc.fr
- **Is there an erratum?**
No. There is no erratum for our initial release. Errata will be documented as future releases on the dataset web page.
- **Will the dataset be updated (e.g., to correct labeling errors, add new instances, delete instances)?**
Additional satellite imagery and ALS-derived height maps may be added to future versions of the Open-Canopy dataset.
- **If the dataset relates to people, are there applicable limits on the retention of the data associated with the instances (e.g., were individuals in question told that their data would be retained for a fixed period of time and then deleted)?**
N/A..
- **Will older versions of the dataset continue to be supported/hosted/maintained?**
Yes. We are dedicated to providing ongoing support for the Open-Canopy dataset.
- **If others want to extend/augment/build on/contribute to the dataset, is there a mechanism for them to do so?**
Proposed extensions or corrections to the Open-Canopy dataset may be submitted to the providers for consideration. The providers will assess the feasibility of incorporating the suggested modifications, considering factors such as data licensing, maintenance requirements, and relevance.
- **Any other comments?**
No.